Why Blood Pressure and Body Mass Should be Controlled for in Resting-State Functional Magnetic Resonance Imaging Studies

Guro Stensby Sjuls

MAPSYK360,

Masters Program in Psychology:

Behavioral Neuroscience

at

UNIVERSITY OF BERGEN

FACULTY OF PSYCHOLOGY

SPRING 2020

Word Count: 18 636

Main supervisor: Karsten Specht,

Department of Biological and Medical Psychology, University of Bergen

Abstract

Replicability has become an increasing focus within the scientific communities with the ongoing "replication crisis" in psychological and medical research. One area that appears to struggle with highly unreliable results is resting-state functional magnetic resonance imaging (rs-fMRI). Therefore, the current study aimed to improve the knowledge of possible contributing factors to this tendency. Arterial blood pressure, body mass, hematocrit, and glycated hemoglobin were investigated as potential sources of between-subject variability in rs-fMRI, in healthy individuals, as previous research has indicated that these variables could affect the results of these studies. Whether changes in resting state-networks (rs-networks) could be attributed to variability in the BOLD-signal, changes in neuronal activity, or both, was of special interest. Within-subject parameters were estimated utilizing Dynamic Causal Modelling as it allows hemodynamic and neuronal parameters to be modeled separately. The hemodynamic parameters were modelled to describe aspects of the BOLD-signal, and the neuronal activity was modelled as effective connectivity, namely the causal interference one region has over other regions within the networks. The results of the analyses imply that blood pressure and body mass can cause between-subject and between-group variability in the BOLD-signal and that all the included factors can affect the underlying connectivity. Given the results of the current and previous studies, the rs-networks, in particular the Default Mode Network, appear to be susceptible to a range of factors, which is likely to contribute to the low degree of replicability of these studies.

Keywords: Resting-state functional magnetic resonance imaging, resting-state network, dynamic causal modelling, blood pressure, body mass, hematocrit, glycated hemoglobin

Sammendrag

Replikasjonskrisen innen psykologisk og medisinsk forskning har gitt de vitenskapelige miljøene et økt fokus på replikasjon av forskningsresultater. Et område der mange av resultatene virker å ha lav reliabilitet, som gjør funnene utfordrende å replikere, er innen funksjonell magnetresonans-avbildning hos hvilende individer (hvile-fMRI). Derfor var målet med denne studien å øke kunnskapen om hvilke faktorer som potensielt bidrar til denne tendensen. Arterielt blodtrykk, kroppsmasse, hematokrit og glykert hemoglobin ble undersøkt som mulige kilder til mellom-subjekt variabilitet i hvile-fMRI, hos friske individer, ettersom tidligere studier har indikert at disse faktorene kan påvirke resultatene fra denne typen studier. Om endringer i hvile-nettverk kan attribueres til variabilitet i BOLD-signalet, endringer i nevral aktivitet, eller begge, var av spesiell interesse. Dynamic Causal Modelling ble benyttet for å estimere innen-subjekt parametere, ettersom teknikken muliggjør separat modellering av hemodynamiske og nevrale parametere. De hemodynamiske parameterene modelleres som beskrivelser av ulike aspekter ved BOLD-signalet, og de nevrale parameterene modelleres som effektiv konnektivitet, altså den kausale påvirkningen et hjerneområde har over et annet område. Resultatene av analysene indikerer at blodtrykk og kroppsmasse kan føre til mellom-subjekt variabilitet i BOLD-signalet, og alle de inkluderte faktorene kan påvirke den underliggende konnektiviteten i hvile-nettverkene. Gitt resultatene av denne og tidligere studier, virker det som at hvile-nettverk, spesielt Default Mode Network, er mottakelige for å bli påvirket av en rekke faktorer. Dette bidrar trolig til den lave graden av reliabilitet i disse studiene, som kan føre til at resultatene er vanskelige å replikere.

Nøkkelord: Funksjonell magnetresonanstomografi, hvilenettverk, dynamic causal modelling, blodtrykk, kroppsmasse, hematokrit, glykert hemoglobin

Acknowledgements

There are many to thank for their help and support in the process of writing this thesis. Firstly, a big thank you to my supervisor, Prof. Karsten Specht. I´m especially grateful for the willingness to supervise both my master thesis and student research scholarship; I've had the feeling that my thoughts and decisions have been supported, and that means a great deal to me. Maybe I'll eventually come to understand more of the *Free Energy Principle*, but in the meantime, thank you for seemingly not growing tired of explaining. I´d also like to thank everyone in the Re:State-research group for letting me participate in their meetings and fun.

My friends, everyone who has ever lived in Klostergaten, my class mates, and, to highlight a few; Marie and Anne Marte. Also, many thanks to my big family, especially my brothers for keeping me grounded and not letting me think of myself as a "neuroscientist or something". To my parents, for not really understanding how my studies in psychology won't turn me into a therapist at some point, but supporting me either way.

Specific to the writing process, I'd like to send extra thanks to Anna, for her support, friendship and obsession with APA-style. Vanessa, for her good advice and inspiring working morale. Petter, for distracting me with discussions about everything that has absolutely nothing to do with the master's thesis. Aslak, for providing me with a home office, and for keeping it sanitized at all times. And to Synnøve, simply for being my best friend for a really long time, and for keeping my head over the (rainy) water while living in Bergen.

Data were provided by the Human Connectome Project, WU-Minn Consortium (Principal Investigators: David Van Essen and Kamil Ugurbil; 1U54MH091657) funded by the 16 NIH Institutes and Centers that support the NIH Blueprint for Neuroscience Research; and by the McDonnell Center for Systems Neuroscience at Washington University.

Abbreviations

rs-fMRI: Resting State Functional Magnetic Resonance Imaging

rs-Network: Resting State-Network

BP: Arterial Blood Pressure

Dia BP: Diastolic Blood Pressure

Sys BP: Systolic Blood Pressure

BMI: Body Mass Index

HCT: Hematocrit Levels

HbA1c: Glycated Hemoglobin

oHb: Oxygenated Hemoglobin

dHb: Deoxygenated Hemoglobin

CBF: Cerebral Blood Flow

rCBF: Relative Cerebral Blood Flow

CBV: Cerebral Blood Volume

BOLD-signal: Blood Oxygen Level Dependent Signal

ROI: Region Of Interest

ICA: Independent Component Analysis

DCM: Dynamic Causal Modelling

csd: Cross-Spectral Density

DMN: Default Mode Network

CEN: Central Executive Network

SN: Salience Network

PCC: Posterior Cingulate Cortex

mPFC: Medial Prefrontal Cortex

LIPC: Left Inferior Parietal Cortex

RIPC: Inferior Parietal Cortex

DLPFC: Dorsolateral Prefrontal Cortex

PPC: Posterior Parietal Cortex

AI: Fronto-Insular Cortex/Anterior Insula

ACC: Anterior Cingulate Cortex

HCP: Human Connectome Project

Table of Contents

The background for this study is the ongoing replication crisis in the field of psychological research (Maxwell, Lau & Howard, 2015). It has been proposed that as few as 39% of published psychological research can be replicated (Collaboration, 2015). Multiple factors are believed to contribute to this tendency, as a pressure to report significant results prevents non-significant results from being published, causing researchers to search for significant results in their datasets rather than testing hypotheses (Sætrevik & Peterson, 2017). In addition, countless studies in neuroimaging have low statistical power due to small sample and effect sizes, which contributes to low replicability (Button et al., 2013; Turner, Paul, Miller & Barbey, 2018). This tendency is also evident in resting-state functional magnetic resonance imaging (rs-fMRI), where the brain functions of resting individuals are being studied. Even so, the interest in rs-fMRI has increased, evidently through the impressive growth of the papers published during the last decades (Biswal, 2012).

The growth of rs-fMRI studies can, in part, be explained by the identification of resting-state networks (rs-networks). Namely, that the activation under the resting condition can be organized into consistent networks and that changes in these can occur following, or as a part of, several neurological diseases and states (Snyder & Raichle, 2012). Shorter scanning times are required, compared to traditional task-based fMRI, which cuts costs, and this economic incentive might also contribute to the popularity and growth of rs-fMRI as a neuroimaging technique (Murphy, Birn & Bandettini, 2013).

Even as rs-fMRI is a popular technique, the results seem to show a high degree of between- and within-subject variability with a variety of endogenous and exogenous factors. Mapping these factors and their effect on the results could improve the reliability, which is especially important when investigating whether rs-fMRI could be applied as a clinical tool (Specht, 2019).

The aim of this study was therefore to investigate the effect that some endogenous factors have on the hemodynamics and neuronal activity of three large-scale rs-networks. The endogenous factors were arterial blood pressure (BP), body mass (BMI), hematocrit levels (HCT), and glycated hemoglobin levels (HbA1c). These are chosen as they might affect the blood supply to the brain, which could affect the BOLD-signal that is measured with fMRI, in addition to having been shown to affect the neuronal activity of the rs-networks. This study aimed to clarify whether these factors could explain between-subject and between-group variability in rs-fMRI results, and whether this variability could be attributed to cerebral hemodynamics, neuronal activity, or both.

Variability in Resting-State Functional Magnetic Resonance Imaging

To introduce how endogenous factors related to the circulatory system potentially can cause variability in rs-fMRI results, a brief overview of the circulatory system and the blood transportation to the brain will be given, in addition to how the properties of the blood vessels can affect the blood flow. Further, there will be given an account of how blood flow relates to neuronal activity, how the fMRI-technique can be used to measure this activity, and how the activity can be modeled, especially in terms of effective connectivity and hemodynamic response. Lastly, how the results from rs-fMRI are affected by BP, HCT, BMI, HbA1c, and why this is a problem related to the replication crisis, will be described.

The Circulatory System

The cells of the body need oxygen (O_2) to function, and the O_2 is transported by means of erythrocytes (red blood cells), bound to the hemoglobin complex of the cell. The oxygenated blood (oHb) is transported in the circulatory system, to be utilized in cell metabolism throughout the body. After O_2 is used, the circulatory system transports the deoxygenated blood

(dHb) away from the cells and back to the heart and the lungs for oxygenation (Snyder & Sheafor, 2015). The combined effort of the respiratory and circulatory systems enables the intracellular reactions where organic molecules, like glucose, are oxidized so that water and energy in the form of adenosine triphosphate (ATP) are created. Without O_2, the cascade of chemical reactions that enables the utilization of glucose as an energy supply will cease, and as a result, the cells will die (Pittman, 2011).

The blood vessels. The peripheral vascular system consists of the blood vessels outside of the heart, and constitute a closed system for blood transportation. The vessels are categorized into arteries, capillaries, and veins. The arteries can be further divided into (1) the aorta, which is the main artery that transports blood out of the heart, and (2) the arteries, which branch into (3) the arterioles. Collectively these vessels transport oHb to the tissue, after the blood has been oxygenated. The arterioles distribute oHb to the smallest blood vessels; the capillaries, where the gas exchange between the vessels and the tissue occurs (Tucker & Mahajan, 2018).

The capillaries are narrow which increases the resistance and causes the blood to flow slower, enabling the exchange of gases and nutrients (Pittman, 2011). The capillaries of the nervous system mostly consist of continuous capillaries, which are covered in a continuous layer of endothelial cells. Intracellular clefts separates the endothelial cells, and it is mostly through these clefts that the exchange of O_2, CO_2, and nutrients can occur (Stephens & Stilwell, 1969).

When oHb is utilized, it is transported to the veins in a more deoxygenated form, and the veins bring dHb back to the heart and lungs. The smallest veins, called the venules, gather the blood from the capillaries and direct it to the bigger veins, which direct the blood back to the heart. In addition, the veins have a storage function; the venous compartments store oHb that is mobilized when nearby cells require it and is adjusted to the need of the body. The veins

store around 50-60 % of the total peripheral blood volume, and if the blood volume increases, more blood is stored here (Attinger, 1969).

Transportation of Oxygen to the Human Brain

As with blood supply to the peripheral tissue in general, the arteries, capillaries and veins cooperate to ensure blood flow. The neurons of the brain consume around 20% of the available oHb, to maintain normal functioning (Clark & Sokoloff, 1999). The cerebral blood flow (CBF) is the blood perfusion to the brain in a given period of time, and the cerebral blood volume (CBV), is the volume of blood in a given amount of brain tissue. Keeping these factors relatively stable is critical for survival, as they support the brains high metabolic demand (Cipolla, 2009).

The cerebral vasculature that transports blood to and within the brain, is a complex system of blood vessels, connected in a manner that supports a constant and stable blood perfusion (Payne, 2016). Some large arteries are transporting oHb from the heart, to be distributed to different parts of the brain through arteries and arterioles, and there is also an intricate system of veins for transporting dHb from the brain to the heart (Stephens & Stilwell, 1969).

Arteries. The aorta branches into the vertebral artery, that in collaboration with the basilar artery ensures CBF to the brain stem and cerebellum. The basilar artery forms an artery circle, joint with two internal carotid arteries. This circulus arteriosus, often known as Willis Circle, is located around the optic chiasma, and forms the starting point for the arteries that supply the rest of the brain with oHb (Stephens & Stilwell, 1969).

The posterior cerebral artery transports oHb to the posterior part of cerebrum, and to the occipital and parietal lobes. The medial cerebral artery runs along the temporal lobe, in the sylvian fissure, and supports the temporal lobes, as well as lateral parts of the frontal and parietal

lobes, with oHb. The anterior cerebral artery runs as two arteries to the frontal lobe, supporting blood flow to the frontal parts of the brain. Jointly, the posterior cerebral artery and the anterior cerebral artery supports blood flow to the medial parts of the brain (Sand, Sjaastad, Haug & Bjålie, 2018).

Veins. To bring dHb away from the capillaries, the venules transports dHb to the bigger veins. The veins of the brain are wide, and without vein-valves. They can be divided into four groups; superior cerebral veins, inferior cerebral veins, middle cerebral veins, and the great cerebral vein. The blood is drained from the veins to vein sinuses in the dura mater of the meninges, along with cerebrospinal fluid (CSF) from the subarachnoid space (Schmidek, Auer & Kapp, 1985; Stephens & Stilwell, 1969) The veins, respectively, drain into the superior sagittal sinus, the transvers sinus, the cavernous sinus, and the straight sinus. The largest sinus vein, the superior sagittal sinus, lies between the two hemispheres, along falx cerebri (Stephens & Stilwell, 1969). Most of the dHb is transported back to the heart through the internal jugular vein (Schmidek et al., 1985).

Regulation of cerebral blood flow. The mechanisms ensuring stable CBF are regulated by outer mechanisms, as well as the brain's independent regulation. In both instances, the characteristics of the blood vessels play a central part. The arteries and veins of the brain, like most of the blood vessels of the body, consist of an inner, a middle, and an outer layer. The middle layer consists of smooth musculature, enabling the vessels to contract and expand, depending on the thickness of the layer. The thickness varies between the vessels, and thereby affects the vessels vascular reactivity and ability to influence CBF (Siegel, 1996).

The arteries have a relatively thin layer of smooth musculature, therefore their contractions only modestly changes the diameter of the vessel. In the arterioles, the smooth musculature is of greater importance, and the layer is therefore thicker. When the arterioles contract the segmental vascular resistance increase, which reduces the CBF (Faraci & Heistad,

1990; Furchgott, 1983; Siegel, 1996). The venules have a thin layer of smooth musculature, compared to the walls of the veins, that has a relatively thick layer of smooth musculature. This enables the veins to contract, to utilize the oHb of the CBV of the venous compartments, which increases the arterial blood volume (Tucker & Mahajan, 2018). As mentioned, the regulation of contraction and relaxation of the smooth musculature is under hormonal and sympathetic nervous control, as well as being controlled by cerebral autoregulation (Walsh, 1994).

Cerebral autoregulation. As it is crucial for the brain to maintain a stable perfusion pressure at all times, cerebral autoregulation enables the brain to adjust the diameter of the arterioles and veins independent of nerves and hormones from the outside. As with regulation of CBF in general, the elasticity and smooth musculature of the blood vessels enables vascular reactivity; contractions increases the segmental vascular resistance which decreases CBF, and the dilation decreases the segmental vascular resistance which increases CBF (Strandgaard & Paulson, 1984). Several mechanisms account for the cerebral autoregulation, including myogenic regulation and cerebral metabolic regulation.

Myogenic regulation enables stable perfusion pressure when the arterial blood pressure (BP) is moderately changed, e.g. when moving from a lying to a standing position. This mechanism is beneficial as the range of factors that can change the BP, like physical activity, does not change CBF to a large degree. It also enables the mobilization of oHb from CBV in the venous compartments, for example if an individual is losing large amounts of blood (Tan, Hamner & Taylor, 2013).

Cerebral metabolic regulation, however, ensures increased perfusion pressure to brain regions that are relatively more active, ensuring relative CBF (rCBF). This is linked to the neural activity, as the regions involved in a specific brain function requires increased amounts of oHb (Lassen, 1959). Nitric oxide has been proposed as a possible communicator between the neurons and the endothelial cells of the blood vessels; acting as a vasodilator (Bredt, Hwang

& Snyder, 1990). However, the exact neurovascular mechanism that enables the vessels to dilate to meet the energy demand of a given neuron is poorly understood (Gauthier & Fan, 2019). Still, this metabolic autoregulatory mechanism, and its subsequent increase in CBV, is what is utilized when the fMRI-technique is used to study the localization of brain functions (Ogawa, Lee, Kay & Tank, 1990).

Functional Magnetic Resonance Imaging

From its development around the 1980s, the non-invasive functional magnetic resonance imaging (fMRI) technique has become a widely used tool for acquiring insight into functionally specialized brain areas. By utilizing hemodynamic changes related to blood metabolism, neuronal activity is measured (Heeger & Ress, 2002).

The fMRI technique is based on the stable and strong magnetic field created by the large magnet of a magnetic resonance (MR) scanner, and utilizes the differences in magnetic susceptibility of oHb and dHb. By using a MRI sequence that is sensitive to these small magnetic differences, it is possible to measure changes in blood oxygenation. Accordingly, the contrast between oHb and dHb is called the blood-oxygen-level-dependent (BOLD)-signal/contrast (Gauthier & Fan, 2019).

The MRI technique. When entering a MRI scanner, the participant is exposed to the main magnetic field of the scanner. The strength of the magnet makes the magnetic moments of the protons of the body's hydrogen atoms align with the magnetic field, as the protons are positively charged. To disrupt this equilibrium state, and create a signal that can be detected, a rotating magnetic field, consisting of gradient coils, is applied along the axis of the main magnetic field. This exerts the hydrogen protons and shifts the net magnetization from the longitudinal plane, which the protons are primarily aligned along, to the transverse plane. The transverse component of the system is normally zero when the net magnetization is aligned with

the longitudinal component, but it is only the transverse component that is measured with MRI technology (Ogawa et al., 1990; Zeidman, Jafarian, Corbin, et al., 2019).

When the rotating magnetic field is turned off, the transverse component proceeds to precess around the main magnetic field. This process, where the transverse component of the net magnetization is reduced, is characterized by an exponential decay with a time constant T_2*. The process is often called effective transverse relaxation, and any spatial variation in the amplitude of the magnetic field within one voxel will lead to differences in the frequency of the precession of the protons. This induces an accumulative decay of the protons, relative to each other, and this relative difference will increase over time (Ogawa et al., 1990; Zeidman, Jafarian, Corbin, et al., 2019).

The BOLD-signal. Oxygenated hemoglobin (oHb) is diamagnetic, which means that it exhibits a weak response to a magnetic field, whereas deoxygenated hemoglobin (dHb) is paramagnetic, exhibiting a stronger response. When a task is performed, cerebral metabolic autoregulation ensures a higher rCBF to the regions that are functionally involved in the given task. As the oHb is utilized, the activity will cause a temporary and local increase in dHb. Nearby arterioles dilate, increasing the rCBF, to meet the need for additional oxygen in the given area and compensate for the high concentration of dHb. The concentration of dHb is weakened, resulting in a more stable magnetic environment and slower dephasing of the transversal magnetization (T2*) than in the initial dip in signal intensity due to the relatively high concentration of dHb (Gauthier & Fan, 2019; Ogawa et al., 1990). The weakened T_2*-weighted signal from dHb is essential to the BOLD-signal, as it affects the proton signaling from the hydrogen atoms in tissue close to the blood vessels (Ogawa et al., 1990; Zeidman, Jafarian, Corbin, et al., 2019).

The BOLD-signal is then analyzed; contrasting a condition with a baseline condition. The differences between brain regions are interpreted as relative differences in neuronal activity

and are used to give indications on regions functionally involved in the performed task (Ogawa et al., 1990).

Dynamic models of the BOLD-signal. Given that the BOLD-signal is an indirect measure of neuronal activity, that is based on the assumption that a region with higher neuronal activity is in need of increased rCBF, it is likely that endogenous factors related to the respiratory and circulatory system might affect the hemodynamic response of the BOLD-signal in some way (Gauthier & Fan, 2019). So, even though the signal is *related* to neuronal activity, it arises from a combination of changes in CBF, CBV, and oxidative metabolism to meet the energy demands of the active brain (Gauthier & Fan, 2019). Therefore, other factors that can contribute to changes in CBF and CBV, e.g. arterial blood pressure, body mass and fat, and the velocity of the blood, might impact the BOLD-signal, and in turn the fMRI-results (Buxton, Wong & Frank, 1998).

Some mathematical models of the hemodynamic response have been proposed to better understand and make predictions about the relationship between neuronal and hemodynamic responses. Among these are the non-linear Balloon model (Buxton et al., 1998), which describes the dynamics of CBV and dHb. It treats the venous compartments as a balloon, that inflates due to increased CBF. The CBV therefore increases, and as a consequence dHb is released at a faster rate. In turn, this affects the BOLD-signal, essentially prolonging it (Buxton, Uludağ, Dubowitz & Liu, 2004). Factor that can affect CBV and CBF, like BMI and BP, are put forward in the model as affecting the BOLD-signal (Buxton, 2012).

Task-based vs. resting-state fMRI. To make a contrast between a task and when the participant is resting in the scanner, as described above, is the traditional task-based approach to fMRI. Here, the resting condition is viewed as a baseline; a control condition to contrast the task condition against (Heeger & Ress, 2002). However, task activation increases the consumption of energy by only 0.5-1.0%, while the resting condition, or baseline, stands for

60-80% of the brain's total energy consummation (Raichle & Mintun, 2006). The intrinsic activity that the energy consumption represents, is hypothesized to support communication among neurons in the absence of a specific task. The frequency of this energy consumption fluctuates in a range below 0.1Hz (Biswal, Zerrin Yetkin, Haughton & Hyde, 1995; Raichle & Mintun, 2006)

In a protocol for resting-state fMRI (rs-fMRI) studies, where the amplitude of these low-frequency fluctuations (LFF) is measured, the participants are told to have their eyes closed, open, or fixated on a grey cross on a dark screen, and rest in the MR scanner. Measuring the LFF of the BOLD-signal that occurs in this condition is the basis for rs-fMRI procedures, and it is assumed to reflect the intrinsic processes of the brain (Snyder & Raichle, 2012). In addition, the measured time-series of the fluctuations can be analyzed and organized into fairly consistent networks (Allen et al., 2011).

Connectivity of the Resting Brain

By investigating connectivity between and within regions of the brain, consistent resting-state networks (rs-networks) can be observed (Allen et al., 2011). The networks can be derived from the resting condition itself or be based on brain regions that are known to be functionally involved in specific tasks. In the case of the latter, the LFFs of the BOLD-signal in these regions are measured with the rs-fMRI paradigm. rs-networks have been extensively studied over the last two decades, and have been linked to many aspects of human functioning, including various types of neurological diseases, like Alzheimer's disease and depression (Greicius, Krasnow, Reiss & Menon, 2003). Essentially, these studies have given insight into how the activity of the brain act in the absence of a task, and how this activity can change under various conditions (Buckner & DiNicola, 2019).

Analyzing resting state fMRI-data. There are different methods for analyzing data from rs-fMRI, which can be used to identify which regions are functionally or effectively connected. Functional connectivity within or between rs-networks refers to the correlation between regions with simultaneous activity at rest, indicating that these regions are cooperating in a network; being functionally linked. Effective connectivity does in addition indicate the relationship between the regions; it gives insight into the directionality of the communication within or between the regions of the rs-networks (Friston, Harrison & Penny, 2003). In addition, the structural connectivity of rs-networks can be studied, in an attempt to map the underlying "connectome" of the brain (Azevedo et al., 2009; Herculano-Houzel, 2009).

When investigating the underlying functional or effective connectivity of the resting brain, different approaches can be used. These include seed-based analysis, independent component analysis (ICA), and dynamic causal modelling (DCM) (Beckmann, DeLuca, Devlin & Smith, 2005; Biswal et al., 1995; Friston, Kahan, Biswal & Razi, 2014).

Functional connectivity. Seed-based analysis requires predefined Regions of Interest (ROI). The ROIs are then used to calculate correlations within the same time-series, for one or more brain regions. The seed-based ROI approach is therefore useful for testing hypotheses about the relationship among brain regions (Lee, Smyser & Shimony, 2013). ICA, on the other hand, is a data-driven approach that determines the most independent networks based on the BOLD-signal time-series. The number of networks that the analyses are going to determine is decided beforehand (Beckmann et al., 2005; Calhoun, Adali, Pearlson & Pekar, 2001).

Both ROI and ICA can generate measures of functional connectivity, which is thought to reflect how different regions coactivate to maintain a brain function, measured as their synchronization the LLF of the BOLD-signal across regions. Friston et al. (2014) define functional connectivity as the statistical dependencies among observed neurophysiological responses. Using functional connectivity to investigate rs-networks has given great insight into

how the brain is organized. However, it is merely based upon correlations, and cannot be used to infer the causal relationship between neuronal systems, e.g. how activity in one region mediates activity in another region (Friston et al., 2014; Greicius et al., 2003).

Effective connectivity. DCM can be used to estimate effective connectivity, which models the direct causal influence one region of the brain exerts over another (Friston et al., 2003; Zeidman, Jafarian, Corbin, et al., 2019). DCM uses the BOLD-signal time-series from the regions defined with ROI analysis or ICA, and is a data-driven approach. One can argue that DCM provides a better model of actual neuronal activity in the brain compared to functional connectivity, as it is based on Bayesian statistics, which involves incorporating previously known information or theoretical assumptions into the modelling/analyses. In terms of DCM, the relationship between the connections that one wants to study can be incorporated into the modeling. In addition, given the modeling of directionality, DCM makes more causal predictions about the connectivity between regions (Friston et al., 2003; Stephan et al., 2010).

When doing DCM on rs-fMRI data, the frequency domain of the observed functional connectivity can be fitted with the cross-spectral density (csd) of the fMRI time-series, for each predefined region. csd is the correlation of the frequency distribution of the BOLD-signal between brain regions; the signal changes in one region per second is modeled as a function of the csd, namely the activity, in another region. csd-DCM is used with rs-fMRI as the protocol of these studies are not expected to cause any major changes in the BOLD-signal, and it is therefore assumed that the connection strengths remain more or less stable throughout the data acquisition (Friston et al., 2014). Task-based fMRI data, however, is often modeled to the time domain, as a change in the BOLD-signal is assumed to occur following the task (Friston et al., 2014; Zeidman, Jafarian, Corbin, et al., 2019).

In addition to measures of effective connectivity within and between the regions of the rs-networks, csd-DCM extracts parameters of the hemodynamic response, incorporating the

Balloon model (Buxton et al., 2004; Friston et al., 2003; Friston et al., 2014). These parameters are essentially descriptions of the Balloon model; the *transit time* for each region, *decay* as the global parameter of the BOLD-signal, and *epsilon* as the neuronal efficacy (Friston, Mechelli, Turner & Price, 2000). csd-DCM also extracts spectral density values, expressed as α- and β-values, that reflect the amplitudes and exponents of the csd of the neuronal fluctuations (Friston et al., 2014).

Resting-State Networks

Functional, effective and structural connectivity is readily used as a means to study rs-networks (Honey et al., 2009; Park, Friston, Pae, Park & Razi, 2018; Van Den Heuvel & Pol, 2010). Three frequently studied rs-networks are the default mode network (DMN), the central executive network (CEN), and the salience network (SN).

The default mode network. The study of the brain's resting state attracted the attention of the research community of neuroscience in the mid-90s (Biswal et al., 1995). The study of the resting brain led to the discovery of a consistent, functionally connected, pattern of distributed brain regions; as a persistent network of "deactivation". When the participant initiated a goal-directed or attention-demanding behavior or task the activation in the network would cease (Raichle et al., 2001). DMN consists of regions within the association cortex, that are late to develop in humans, and that is thought to have been evolving and expanding with the human evolution (Buckner & Krienen, 2013). The three main hubs or regions of DMN include the precuneus/posterior cingulated cortex (PCC), medial prefrontal cortex (mPFC), and medial, lateral, and inferior parietal cortices (IPC) (Raichle et al., 2001).

There is yet no unified view of the function of DMN, but it has been postulated to support a "default mode" of the brain when an individual is awake and alert, but not actively involved in a task (Raichle et al., 2001). Others have suggested that DMN is involved in a self-

referential and introspective state (Greicius et al., 2003). Studies supporting this theory show that the more the task-demand increases, the more the activity of DMN will decrease, essentially suppressing the network. This might indicate that the attention that in the resting-state can be directed inwards, in demanding tasks will be directed outwards to focus on the extrinsic task (Singh & Fawcett, 2008). There is also some evidence suggesting that DMN is involved in mediating the processes where one retrieves memories, plan for the future, or processing of one's own impressions and feelings (Buckner, Andrews-Hanna & Schacter, 2008). In line with this research, malfunctioning of DMN has been associated with Alzheimer's disease and depression (Greicius, Srivastava, Reiss & Menon, 2004; Hamilton, Farmer, Fogelman & Gotlib, 2015; Mevel, Chételat, Eustache & Desgranges, 2011; Sheline et al., 2009).

The central executive network. As DMN is "deactivated" when a participant is performing a cognitive task, the activation of another network is increasing. The anti-correlation between these networks have been shown to increase with the degree of task difficulty (Fox et al., 2005). CEN is a task-related network, with the predominant regions being the dorsolateral prefrontal cortex (DLPFC), and the posterior parietal cortex (PPC) (Bressler & Menon, 2010; Toro, Fox & Paus, 2008). The neocerebellum also contributes to the function of CEN, as it is believed to contribute to working memory, with the integration of information through cortico-cerebellar loops (Habas et al., 2009).

As mentioned, the nodes of CEN show a strong coactivation during cognitively challenging tasks. It is thought to be involved in the manipulation and maintenance of information in working memory, as well as being involved in decision-making in goal-directed behavior, attention, response inhibition and other executive functions, which qualitatively separates it from DMN (Bressler & Menon, 2010; Koechlin & Summerfield, 2007). Changes in CEN connectivity have been shown to occur with diseases were these functions are altered,

like schizophrenia, borderline personality disorder and with alcohol abuse (Doll et al., 2013; Manoliu et al., 2014; Weiland et al., 2014; Woodward, Rogers & Heckers, 2011).

The salience network. SN has been shown to play a mediating role in up- and downregulating of DMN and CEN (Sridharan, Levitin & Menon, 2008). Some researchers view SN as a part of an attention network, along with the regions of CEN, while others postulate that it plays a specific role regarding attention, that separates it from the rest of CEN (Seeley et al., 2007). The predominant regions of SN are the ventrolateral prefrontal cortex (vlPFC), the anterior insula (AI), and the anterior cingulate cortex (ACC) (Menon & Uddin, 2010)

SN and in particular the insula, is responsive to the degree of salience, and is involved in bottom-up detection of salience; directing attention and memory resources to salient events. It is situated close to regions essential in the cognitive, homeostatic, and affective systems of the brain, which makes it a possible link between stimulus-driven processing and other areas involved in monitoring the internal environment of the brain and body (Craig, 2009; Menon & Uddin, 2010).

Menon and Uddin (2010) suggest that the insula, and more specifically the anterior insula (AI), can be viewed as a central component of SN. They argue that AI is involved in integrating and mediating information flow between different brain networks that are involved in attention processing and cognition, like CEN. According to a study by Sridharan et al. (2008), the fronto-insular cortex and the ACC form a separate network, that is involved in the switching between CEN and DMN, which was tested by investigating the switching between task and resting-state conditions by means of fMRI. ACC also plays a modulatory role in sensory processing and it connects the SN to the supplementary motor cortex. In this matter, ACC is involved in promoting both response selection and motor responses (Crottaz-Herbette & Menon, 2006; Paus, 2001; Rudebeck et al., 2008).

Endogenous Sources of Variability in rs-fMRI

Following the theory of the BOLD-signal and rs-networks described above, the following section will describe how arterial blood pressure (BP), hematocrit levels (HCT), body mass (BMI) and glycated hemoglobin (HbA1c) are related to CBF/CBV. In addition, the results of studies that have found them to be related to changes the rs-fMRI BOLD-signal and/or in rs-network connectivity, will be accounted for. See Appendix A for the description of the literature search.

Arterial blood pressure. To maintain CBF when the resistance increases, for example in smaller vessels or when the blood has a higher viscosity, the pressure of the arteries must increase. The pressure can be measured as arterial blood pressure (BP); the pressure the blood exerts on the arteries (Alexis, 2009; Harper, 1966). Keeping BP within a normal range is especially important for the brain as the mechanisms involved in cerebral autoregulation only function optimally when BP is within a specific range. When BP is too low CBF decreases, potentially damaging the brain tissue, and when BP is too high it can increase the strain on the heart (Harper, 1966). See Table 1 for an overview over what is typically categorized as normal, high and elevated BP.

BP is regulated with information from baroreceptors, which brings information to the cardiovascular center of medulla oblongata. If the center receives information indicating low BP it reflexively initiates a feedback loop, which activates the heart, increasing the strength of its contractions (Harper, 1966). BP is often measured and expressed as systolic and diastolic pressure, namely the pressure the blood exerts on the arteries when it the heart contracts, and the pressure exerted on the arteries while the heart is filling up with blood. Systolic and diastolic BP is commonly measured and expressed in mm/Hg (Alexis, 2009).

Table 1

Blood Pressure Categories

Category	Systolic BP		Diastolic BP
Normal	Less than 120	and	Less than 80
Elevated	120-129		Less than 80
High: Stage I	130-139		80-89
High: Stage II	≥140		≥90
High: Stage III	>180		>120

Note. Criteria for normal, elevated and high (stage I, II, III) blood pressure. The criteria for the given category assumes the combination of the systolic and diastolic arterial blood pressure, as indicated by the "and". BP = blood pressure. Reproduced from Sand et al. (2018).

Mean BP fluctuations are highly coupled with the fluctuations of the BOLD-signal, as it fluctuates around 0.08 Hz. Therefore, a significant component of the BOLD-signal in rs-fMRI seems to have a systemic origin, with around 2.2% of the variance in the BOLD-signal being explained by beat-to-beat mean BP (Whittaker, Driver, Venzi, Bright & Murphy, 2019). By using low-pass filtering, at 0.08 Hz, and applying brain global, white-matter, cerebrospinal fluid mean signal regressions, the spectral power of the BOLD-signal can be reduced by 55.6% to 64.9% (Zhu, Tarumi, Khan & Zhang, 2015). The low frequency fluctuations of mean BP itself might be reflective of an autoregulatory process (Whittaker et al., 2019; Zhu et al., 2015).

The only study, to the best of my knowledge, that has investigated the relationship between functional connectivity of rs-networks and individuals with normotensive BP, studied the relationship with rostroventral medulla. They found this region to exhibit a stronger connectivity to vlPFC, which can be considered a part of SN (Kobuch, Macefield & Henderson, 2019).

Hematocrit. The erythrocytes (red blood cells) transports the O_2 to the brain, and it is the large number of these cells that ensure the velocity of the blood (Stadler et al., 2008). Every erythrocyte contains a large number of hemoglobin molecules (Hb); constituting about 34% of the cell mass. Hb binds O_2 and CO_2, and consists of a globular peptide chain with an ionized iron atom (Fe^{2+}), called globin, and a heme group. Every Fe^{2+} can bind one O_2 molecule, and

this binding is not particularly strong; O_2 is easily bound to the Hb in the lungs, and easily detached from the Hb in the tissues of the body (Krueger & Nossal, 1988; Perutz et al., 1960). The shape and structure give the cells a large surface, to make the O_2 binding more efficient (Smith, 1987).

HCT is the percent wise measure of the blood volume that consists of erythrocytes. As the number of Hb is relatively stable in erythrocytes, HCT is also an indicator of the amount of Hb available and the blood's capacity to transport O_2. If HCT is low the blood will lose some of its ability to transport O_2, and it will have a lower viscosity. However, if the number of erythrocytes is high, the blood is able to transport more O_2 and have a higher viscosity (González-Alonso, Mortensen, Dawson, Secher & Damsgaard, 2006). As mentioned, higher viscosity makes the blood more challenging to transport, and to compensate BP might increase (Jae et al., 2014) . On average, women have lower HCT (42%) than men (45%), due to the male sex hormone testosterone stimulating the production of erythrocytes (Murphy, 2014).

Studies on the relationship between baseline HCT and the BOLD-signal have found it to be contributing to the degree of BOLD-activation. These studies implicate a positive relationship between the BOLD-signal activation and HCT levels, specifically in men. However, the studies used task-based fMRI to investigate the relationship. (Levin et al., 2001; Xu et al., 2018; Zhao, Clingman, Närväinen, Kauppinen & van Zijl, 2007). To the best of my knowledge, no study has yet specifically studied the effect of HCT on the BOLD-signal in rs-fMRI.

In addition, between-subject variations in HCT have been associated with regional differences in connectivity in parts of the DMN, CEN, and SN, namely in ACC, mPFC, intraparietal sulcus, insula, and opercular cortex, by Yang, Craddock, and Milham (2015). The authors point out that it is unclear whether these differences are due to neuronal or non-neuronal variation (Yang et al., 2015).

Body mass. The blood volume makes up around 7% of an average adult's body weight, and it decreases in a non-linear matter with increased body weight (Lemmens, Bernstein & Brodsky, 2006). As a consequence of the amount of body fat rising with age, older individuals have on average a lower blood volume relative to body weight, compared to younger adults (Sand et al., 2018).

Body mass is often calculated using the Body Mass Index (BMI). Based on the equation weight (kg.)/height $(cm)^2$ one can estimate the mass of the body. Normal weight is considered to be a BMI score between 18.5 and 25. A score under 18.5 are considered underweight, and scores over 25 are considered overweight. Scores over 30 are considered obese and scores over 40 are considered severely obese (Kuczmarski & Flegal, 2000). Higher BMI scores are associated with life-style diseases like diabetes mellitus type 2, as well as heart and cardiac diseases (Lam, Koh, Chen, Wong & Fallows, 2015). As BMI affects CBV, it is included in the beforementioned Balloon model, as a factor that might affect the BOLD-signal (Buxton et al., 1998).

Some studies have found decreased within-network connectivity of DMN, CEN and SN, as well as increased between-network connectivity, to be related to higher BMI. However, the results are somewhat varied, as different regions of the rs-networks show altered functional connectivity. According to one study, connectivity of regions within SN (insula/parietal operculum), regions involved in visual processing, and DMN are sensitive to differences in BMI-status. Specifically studying BMI-discordant monozygotic twins, a study found that twins with lower BMI had stronger functional connectivity between striatal/thalamic and prefrontal networks. The twins with a higher BMI, on the other hand, exhibited stronger functional connectivity between DMN and other networks, like a cerebellar network and SN, including the central operculum, and precentral gyrus (Sadler, Shearrer & Burger, 2018).

Similarly, higher BMI has been found to be related to increased functional connectivity between DMN, CEN, a sensorimotor and a visual network, as well as a reduction of DMNs and CENs internal cohesiveness. The authors consider SN a part of CEN, and it is specifically between the frontoparietal part of CEN and SN, and within SN, that they found reduced functional connectivity. However, this study did not find changes in functional connectivity in DMN and CEN when comparing BMI-discordant siblings (Doucet, Rasgon, McEwen, Micali & Frangou, 2017).

Decreased within-network functional connectivity of DMN has also been found between PCC and precuneus in elderly with higher BMI (Beyer et al., 2017), and in the frontal gyrus of DMN in overweight young subjects (Chao et al., 2018). Further, Chao et al. (2018) found increased functional connectivity in ACC bilaterally (parts of the SN), in overweight subjects compared to controls. In contrast to these studies, overweight compared to normal-weight monozygotic female twins did not show altered functional connectivity in DMN, SN, or an ACC-orbifrontal network. After eliminating genetic effects, altered functional connectivity was only seen in a basal ganglia network, specifically within the bilateral putamen (Doornweerd et al., 2017).

The results from these studies on the effect of BMI on rs-networks vary, but several of the authors hypothesize that higher BMI is linked to changes in networks that balance sensory-driven and internally-guided (CEN, DMN) states; this might lead to weight gain as a consequence of poorly regulated eating behavior (Doucet et al., 2017; Sadler et al., 2018).

Glycated hemoglobin. Long-term blood sugar, or glycated hemoglobin, (HbA1c) is a measure related to an individual's glycemic regulation over a period of the last twelve weeks. When blood glucose is regulated in a sufficient way, the HbA1c is normally <5.7% (Chandalia & Krishnaswamy, 2002). High concentrations of glucose in the blood, as a consequence of higher amounts of glucose being bound to the hemoglobin, can indicate a poorly regulated

blood sugar. Therefore, moderately high (5.7-6.5%) and high (>6.5%) scores are indicators of pre-diabetes and Diabetes Mellitus, respectively (Tankova, Chakarova, Dakovska & Atanassova, 2012). As indicated by Iso et al. (1991), HbA1c is a good indication of body fat, measured as hip-waist-ratio. Therefore, HbA1c might be related to blood volume in similar ways to BMI (Lalande, Hofman & Baldi, 2010). However, whether HbA1c levels will affect the BOLD-signal of rs-fMRI is uncertain, as no previous studies have been conducted. A study on the influence of HbA1c levels and BOLD-signaling for stroke patients did not find there to be a relationship between the degree of hemodynamic response with HbA1c, in task-based fMRI (An et al., 2015).

Sadler, Shearrer, and Burger (2019) found no difference in DMN activity between subjects with prediabetes (HbA1c 5.7-6.4) and healthy subjects. They did however find there to be stronger functional connectivity between a ventral attention network, consisting of orbitofrontal cortex and middle temporal gyrus, and a cingulo-opercular network in healthy individuals. This network included insula (part of SN), and DLPFC (part of CEN). The prediabetic subjects did however show stronger functional connectivity between a ventral attention network, a visual and a somatosensory network. The authors discuss whether these differences between groups are associated with differences in self-control, as the functional connectivity of the healthy individuals can be viewed as related to self-control, whereas the functional connectivity of the prediabetic individuals are stronger between areas associated with processing sensory stimuli (Sadler et al., 2019), which resembles the conclusion several authors draw from the previously described BMI results (Chao et al., 2018; Sadler et al., 2018)

Other studies that have investigated the relationship between changes in rs-networks of individuals with type 2 diabetes mellitus compared to healthy individuals, have found diabetic individuals to exhibited weaker functional connectivity in the right insula (part of SN), and from the right insula to the bilateral superior parietal lobule (Liu et al., 2017). The same is seen

in diabetic patients with cognitive impairment, especially in the right insula (Yang et al., 2016). These findings indicate that the insula, in particular, might be affected by higher HbA1c values, or might be involved in the processes leading up to the heightened HbA1c values.

The Replication Crisis in the Field of Resting-State fMRI

As these studies indicate, there are several factors that possibly affect the connectivity and/or the hemodynamic response of the rs-networks. In effect, the rs-variability relates to the ongoing replication crisis in the field of psychological and medical research, as the rs-fMRI studies seem to produce highly varying and unreliable results. The replication crisis has received extended attention and is now acknowledged as an issue by the research community, as outlined in the introduction (Maxwell et al., 2015; Sætrevik & Peterson, 2017).

When conducting rs-fMRI studies specifically, a major problem is that the BOLD-signal show a high degree of within- and between-subject variability, with a range of different factors. This tendency does also, to some degree, apply to task-based fMRI, but these studies have the advantage of a control condition (Specht, 2019). In addition, between- and within-subject variation has been found to correlate with an extensive list of endogenous and exogenous factors. These include the time of year and the time of day, circadian rhythm, sleep duration, prior events, mood, age and gender, to mention only a few (Agcaoglu, Miller, Mayer, Hugdahl & Calhoun, 2015; Choe et al., 2015; Curtis, Williams, Jones & Anderson, 2016; Goldstone et al., 2016; Harrison et al., 2008; Hodkinson et al., 2014; Waites, Stanislavsky, Abbott & Jackson, 2005).

Implications of low replicability. The points mentioned above can be viewed as problems relating to the replication crisis as rs-fMRI evidently is sensitive to varying conditions. As it is challenging to control for all of the factors, the results are in turn difficult

to replicate (Birn, 2012; Duncan & Northoff, 2013; Murphy et al., 2013). This is an issue in itself, which leads to a new set of problems when conclusions are drawn and build on the results.

With the growing interest for rs-fMRI over the last two decades, the technique has been put forward as a potential clinical tool. When rs-fMRI started gaining more interest from the research community, it was partly because it provided an opportunity to investigate the connectivity of the brain in the absence of a task. This was beneficial when studying different clinical groups, as some of the potential issues related to receiving instructions on a task, as well as engage in it, is greatly reduced. As the procedure reviled that alterations of the rs-networks could be observed in these clinical groups it gave rise to the idea of rs-fMRI as a potential diagnostic tool (Specht, 2019). For example, alterations were observed in the DMN of Alzheimer's disease patients, and a substantial amount of research was carried out to investigate whether DMN alterations could be used for diagnosing Alzheimer's disease (Greicius et al., 2004; Mevel et al., 2011). However, they were building on the assumption that the rs-networks are inherently stable across time and within and between subjects, which would make them sensitive to clinical deviations (Specht, 2019). Arguably, the findings indicating that the rs-networks vary with a range of factors gives rise to skepticism about their presumed stability.

Going forward, measures should be taken to better ensure the replicability of these studies. Multi-institutional initiatives collecting big quantities of data, like the Human Connectome Project (HCP) or the UK Biobank, are put forward as potential solutions to the general issue of the replication crisis (Poldrack & Gorgolewski, 2014; U.K, 2014; Van Essen et al., 2013). As they provide large datasets, including rs-fMRI data, it enables researchers to include more subjects in their studies, which contributes to giving the studies higher statistical power (Poldrack & Gorgolewski, 2014). fMRI studies often have a low number of participants which makes the results less reliable (Button et al., 2013). In addition, the data collection of

these initiatives is transparent with available study protocols, which makes it easier for researchers to replicate other studies (Poldrack & Gorgolewski, 2014). Therefore, the data from these initiatives can be used to investigate the effect different factors have on rs-networks and the hemodynamic response in a large sample.

Aims of the Current Study

To further increase the knowledge on between-subject variability in the rs-networks of healthy individuals, the effect of BP, HCT, BMI and HbA1c was investigated. As the previously mentioned studies and theoretical framework indicate, these factors might cause variability in both hemodynamic and neuronal parameters. A research procedure that would allow for functionally separating the BOLD-signal variation that can be attributed to hemodynamics, and the BOLD-signal variation that can be attributed to neuronal activity, was considered as highly relevant:

Firstly, as some of the variation ascribed to variance in neuronal connectivity might in fact be attributable to hemodynamic variance, in which case the conclusions drawn from functional connectivity studies might be flawed. Secondly, if the variables cause variability in both the hemodynamic and neuronal parameters of the BOLD-signal, it would imply that at least some of the variation in the hemodynamic parameters should be accounted for when drawing conclusions on connectivity. Thirdly, if all of the potentially observed variability can be ascribed to the neuronal parameters of the BOLD-signal, it could potentially confirm previous studies on rs-connectivity. And finally, a study that aims to ascribing the potential variability caused by some endogenous factors to either the hemodynamic response independently of neuronal activity, or the neuronal activity in rs-networks, have not previously been conducted. Independent of the direction of the results, if either the hemodynamic response,

the neuronal activity, or both, are affected by the variables included in the current study, it would speak for rs-networks as lacking some of the stability that they are assumed to possess.

The current study therefore aimed at investigating the between-subject variability that BP, HCT, BMI and HbA1c, might cause in rs-fMRI results, as well as the between-group variability potentially caused by BMI, in a healthy population. The overarching implications of the current study mostly relate to the ongoing replication crisis and what measures can be taken to ensure more reliable results in the fast-growing field of rs-fMRI; essentially facilitating more reliable results for future studies.

Research Question and Hypotheses

The following research question was asked: Can between-subject variability in BP, HCT, BMI and HbA1c affect the hemodynamic response and neuronal activity of large-scale rs-networks? The hypotheses under "Hemodynamic response" and "Neuronal activity" were postulated as primary hypotheses, to answer the research question at hand. Notably, large effect sizes were not expected, as previous studies have found a range of other factors to cause variability in rs-fMRI. Therefore, relatively small effect sizes were expected, so that the combination of these and other variables are collectively causing variability in the results of rs-fMRI.

Hemodynamic response. In line with the studies and theoretical framework outlined in the introduction, the following hypotheses were postulated for the effect of the endogenous factors on the dynamics of the rs-fMRI BOLD-signal:

Hypothesis 1 (H_1): Increased BP will weaken the dynamics of the BOLD-signal, as it might represent increased segmental vascular resistance.

Hypothesis 2 (H_2): Increased HCT will strengthen the dynamics of the BOLD-signal, in line with the previously conducted research described above.

Hypothesis 3 (H_3): Increased BMI will weaken the dynamics of the BOLD-signal, as CBV decreases with increased body weight.

Hypothesis 4 (H_4): Increased HbA1c will decrease the dynamics of the BOLD-signal, based on the same principal as with BMI.

Put shortly: Increased BP, BMI and HbA1c was hypothesized to weaken the BOLD-signal, whereas increased HCT it hypothesized to strengthen the BOLD-signal.

Neuronal activity. In line with the studies outlined in the introduction, the following hypotheses are postulated for the effect of the endogenous factors on the connectivity within the rs-networks:

Hypothesis 5 (H_5): Increased HCT will weaken the internal connectivity of DMN, CEN and SN.

Hypothesis 6 (H_6): Increased BMI will weaken the internal connectivity of DMN and SN, and increase the between-network connectivity.

Hypothesis 7 (H_7): Increased HbA1c values will weaken the internal connectivity of CEN and SN, and increase the between-network connectivity.

The relationship between the endogenous factors. In addition, some secondary hypotheses were postulated on the relationship between the study's independent variables:

Hypothesis 8 (H_8): Diastolic and systolic BP are positively correlated.

Hypothesis 9 (H_9): BP and HCT are positively correlated.

Hypothesis 10 (H_{10}): BP and BMI are positively correlated.

Hypothesis 11 (H_{11}): BP and HbA1c are positively correlated.

Hypothesis 12 (H_{12}): HCT and HbA1c are not correlated.

Hypothesis 13 (H_{13}): HCT and BMI are positively correlated.

Hypothesis 14 (H_{14}): BMI and HbA1c are positively correlated.

Methods

Research Design

To test the hypotheses, a between-subject and between-group design was chosen. Firstly, a csd-DCM analysis resulting in within-subject parameters of the hemodynamic response, effective connectivity, cross-spectral density (csd) and Free Energy (model evidence), was conducted. Secondly, how much of the between-subject variance in the hemodynamic and effective connectivity parameters that could be predicted by BP, HCT, BMI and HbA1c was examined. As gender has been shown to affect rs-networks, an analysis that allowed to control for the effect of gender was utilized. Thirdly, the endogenous factor BMI was split into groups for comparison on the hemodynamic and effective connectivity parameters. Lastly, the effect of the independent variables on the csd-DCM parameter Free Energy (model evidence), was examined. This was done to investigate whether including the independent variables in the model increases the model evidence, which could support the idea that the contribution of the variables collectively is contributing to variability in the results.

The study therefore had a hierarchical design, as the first step, namely within-subject estimation of parameters had to be performed prior to the between-subject and between-group analyses. Healthy subjects were studied, to give indications of variability within a normal population. A large sample was aimed for, to ensure statistical power.

After ethical and practical considerations, previously collected data from the Human Connectome Project (HCP) was considered sufficient to answer the research question as they provide data on a large sample of the healthy population, including rs-fMRI data, biological data, and a range of data points from various questionnaires. In addition, the large sample ensures statistical power, which in turn makes the results more replicable; in line with the overarching goal of the study. Thus, no additional data was collected. A smaller subsample was

chosen from the available HCP sample, for reasons related to DCM analyzing time. However, the number of subjects in the study sample were still considerably higher than in conventional rs-fMRI studies, which was aimed for. Information on the subjects and the data collecting protocols are available online, allowing transparency and insight into potential advantages and disadvantages of the data used (HumanConnectomeProject, 2017).

Ethical Considerations

The data was from HCP, which is a partially open-access database. However, access to data of a more sensitive nature is not open to the public. This was specifically applied for and approved by HCP for the current study. This study was approved by the regional ethics comity for medical research, "Regional Etisk Komité for Medisinsk Forskning (REK)", as a part of the project "When Default is not Default" at the institute of Biological and Medical Psychology, University of Bergen. (see Appendix B).

Using already existing data, and thereby not recruiting new participants, is beneficial from an ethical standpoint, as no additional subjects were put through the potential stress of the research procedure (Poldrack & Gorgolewski, 2014). The HCP subjects signed an informed consent document, before doing any further procedures, and all data was anonymized with subject codes, without personal information. The participants consented to their anonymous data being shared; the data containing less sensitive data being shared openly (e.g. fMRI-images), and the data containing more sensitive data (e.g. family history and psychiatric history) being shared with the researchers granted access (Van Essen et al., 2013).

The subsequent guidelines were followed while working with the HCP data in the course of the current study: As the data is from a specific population from a restricted geographical area, it is important to take steps in order to keep the subjects anonymous (Poldrack & Gorgolewski, 2014; Van Essen et al., 2012). Some of the data is of a sensitive matter, for

example regarding the use of alcohol and drugs, as well as psychiatric history. According to the HCP guidelines for restricted data, it should not be shared. This includes storing the data in a safe way, as well as not discussing sensitive data over e.g. email. Researchers that wish to use the restricted data are required to apply for it personally, and therefore the data was only discussed between members of the research group that had been granted access. If the results are to be published, the sensitive data should not be combined in such a way that it could identify the subjects (HumanConnectomeProject, 2013, 2016).

Data Acquisition

Subjects. The section of data that was used in this study stems from a branch of the HCP studying young healthy individuals, the "HCP S1200 release", which was collected over a period of approximately three years (Van Essen et al., 2013).

Recruitment. The subjects were drawn from a population of healthy young adults, born in Missouri. The subjects were recruited on the basis of age and whether they came from a family that included twins, based on the Missouri Department of Health and Senior Services Bureau of Vital Records. The recruited subjects were monozygotic and heterozygotic twins and their non-twin siblings, ranging from 22 to 35 years of age (Van Essen et al., 2013).

Inclusion and exclusion criteria. HCP aimed at recruiting subjects that represent the broad U.S. population, in terms of ethnic, racial, and socioeconomic representation, to reflect the variability that can be found within a population. The same principle was applied to health status, as the study included individuals that were smokers, overweight, or had a history of heavy drinking or recreational drug abuse (Van Essen et al., 2013).

Individuals with severe neurodevelopmental disorders, e.g. schizophrenia, or neurological disorders, e.g. Parkinson's disease, were excluded along with their siblings. Twins born earlier than week 34, and non-twin siblings born earlier than week 37, were excluded.

Interestingly, in the case of this study, individuals with diabetes, and high BP were excluded; "as these might negatively impact neuroimaging data quality". However, subjects with undiagnosed high BP and diabetes kept under control by means of diet were included in the study (Van Essen et al., 2013). See Appendix C for a full overview of inclusion and exclusion criteria.

Phone interviews were used to inquire if the participants met the inclusion and exclusion criteria. If a minimum of three family members, including one twin pair, met the criteria and were willing to participate, they were given a longer phone interview; the Semi-Structured Assessment for the Genetics of Alcoholism (SSAG) (Bucholz et al., 1994). This assessment was used to make sure that the subjects did not have any significant psychiatric illnesses (Van Essen et al., 2013).

Study sample. The total number of subjects in the HCP Healthy Young Subjects "S1200 release" is 1206, which of a subsample was used in the current study (N=594) (Van Essen et al., 2012) A smaller sample was chosen as it cuts analyzing time, as the DCM analysis can be fairly time-consuming. To obtain the within-subject parameters with this smaller study sample, the DCM analysis was running for around 3 weeks. The sample was semi-randomly chosen, on the basis of an equal distribution of gender and age, as a part of another study.

Behavioral and biological testing. After completing the phone interview, the subjects spent two days at the research facility (Washington University, St. Louis, Missouri, U.S.), and a set of behavioral assessment tests were performed (see Appendix D for the full list of behavioral and biological tests) (Van Essen et al., 2013).

Blood samples for HCT and HbA1c to assess the percentage of red blood cells and glycemic regulation over time. The blood samples for these tests were drawn at some point during the two days (HumanConnectomeProject, 2018). For HCT, blood samples were drawn two times. The data from the first draw was used in this study.

Weight and height were self-reported by the subjects, and a BMI score was calculated using the equation height/weight^2 (kg./m^2). As mentioned, CBV is decreased with increased weight. However, as BMI takes the height of the subject into account, it was considered a more convenient measure. In addition, Buxton's Balloon model explicitly mentions BMI as a factor that might affect the dynamics of the BOLD-signal (Buxton, 2012; Van Essen et al., 2013).

BP was obtained for each subject. Conventionally, the BP consist of two variables; systolic and diastolic BP (HumanConnectomeProject, 2018; Van Essen et al., 2013). HCP does not report exactly how BP was measured. Assuming a conventional manual BP apparatus was used, the BP was measured using a cuff around the upper arm, at the same height as the heart. The cuff is filled with air, which stops the blood flow to the arm. When the blood flow is completely restricted, the pressure caused by the cuff is slowly released. While listening to the blood flow with a statoscope, the systolic BP is measured when the blood is flowing back to the arm, making a turbulent sound. The diastolic BP is measured when the blood flows freely; when the turbulent sound ceases. If an automatic BP apparatus was used, the same principle applies, but the measures are taken automatically (Sand et al., 2018).

Scanning protocol. The subjects were scanned with a customized Siemens 3T "Connectome Skyra" at Washington University. The scanner included a 32-channel head coil, custom gradient coils and gradient power amplifiers that increase the gradient strength from 40 mT/m to 100 mT/m. Using the customized gradient set also resulted in a smaller diameter of the inner bore of the scanner than on a standard Siemens 3 T Skyra. Prior to the first scan, subjects underwent a practice scan in a mock scanner, to be accustomed to the scanning environment and to get feedback on head motion (Uğurbil et al., 2013; Van Essen et al., 2013; Van Essen et al., 2012).

Based on piloting, a protocol was established to acquire the rs-fMRI data, which used a gradient-echo multiband EPI imaging sequence. The rs-scans, which over the time of the two-

day visit lasted for a total of 1 hour (2 x 15 min per day), were acquired with opposite encoding directions; from left to right (L/R) and from right to left (R/L). The participants were instructed to leave their eyes open, fixating on a cross-hair during the scans. To address the potential problem of head motion, information on dynamic head motion and position was gathered, using an optical motion tracking camera system (Moire Phase Tracker, Kineticor). A computer displayed the head motion in real-time, and the information generated was stored in a data file, linked to the scan it was associated with (Van Essen et al., 2013).

Image Acquisition. To obtain high resolution T1-weighted structural MR images, the following settings were applied: Repetition Time (TR) 2400ms, echo time (TE) 2.14ms, inversion time (TI) 1000ms, flip angle of 8°, field of view (FOV) 224 x 224mm (readout x phase encoding), 0.7mm isotropic voxels, and a multiband factor of 8 (Uğurbil et al., 2013).

The settings for the rs-fMRI were: TR of 720 ms, TE of 33.1 ms, 52° flip angle, FOV 208mm x 180mm, slice thickness 2.0mm; 72 slices; 2.0 mm isotropic voxels and a multiband factor of 8 (Uğurbil et al., 2013).

Image Processing. Unprocessed fMRI images are normally preprocessed before they are analyzed as they contain a range of spatial distortions, are not in a standard anatomical space, and are misaligned across modalities. In addition, noise, artifacts and biases need to be corrected for, before the statistical analysis can be conducted. For rs-fMRI this includes de-noising, and removal of motion confounds, as well as brain parcellation, and network analysis (Glasser et al., 2013).

HCP optimized the preprocessing to compensate for the spatial distortions, at the same time as minimizing the loss of data, in the "HCP Minimal Pre-processing Pipeline". Using the "Connectome Skyra" scanner, with a smaller bore (56cm) than a conventional scanner, resulted in the participants heads not being centered along the gradient isocenter, which needed to be corrected for as all the scans had gradient distortions greater than a conventional scanner, e.g.

a Siemens 3 T Skyra. In the minimally pre-processed data, which was used in this study, these distortions were already corrected (Glasser et al., 2013; HumanConnectomeProject, 2018).

The additional preprocessing of the data included smoothing with a 6mm Gaussian kernel. To regress out non-grey matter sources of noise in the data, from white matter and cerebrospinal fluid, a region of interest (ROI) was specified for each. To control for subject movement in the course of the scanning session, twelve movement parameters were included in the analysis.

Statistical Analyses

To study the effect of BP, HCT, BMI and HbA1c on the hemodynamics and effective connectivity in rs-networks, the rs-fMRI time-series from eight regions of interest (ROIs) where extracted, using the HCP "S1200 release" data that was already preprocessed with the "HCP Minimal Pre-Processing Pipeline" (HumanConnectomeProject, 2017). Cross-spectral density DCM (csd-DCM) was used to extract the cross spectral density (csd) from the time-series of each ROI; estimating within-subject parameters. The hypotheses were then tested on the DCM parameters with the data for each subject on BP, HCT, BMI and HbA1c, which was available from the HCP database. The ROI extraction and time-series extraction was performed in MATLAB and in the MATLAB extension SPM12 (version 2018a). Hierarchical linear regression analyses and a test of between-group variance were performed for the hypothesis testing, in IBM SPSS Statistics (Version 25).

Within-Subject Estimates

ROIs for each rs-network for each subject was specified from the preprocessed HCP "S1200 release" data, for the study sample (N=594). Eight ROIs were extracted, including four

regions from DMN, two regions from CEN and two regions from SN. See Table 2 for the coordinates for each region and which network they are a part of.

Table 2

Coordinates for Regions of Interest

Resting State Network	Regions	R/L	MNI Coordinates
Default Mode Network	Posterior Cingulate Cortex	R/L	0 -52 26
	Medial Prefrontal Cortex	R/L	3 54 -2
	Left Inferior Parietal Cortex	L	-50 -63 32
	Right Inferior Parietal Cortex	R	48 -69 35
Central Executive Network	Dorsolateral Prefrontal Cortex	R	45 16 45
	Posterior Parietal Cortex	R	54 -50 50
Salience Network	Fronto-Insular Cortex	R	37 25 -4
	Anterior Cingulate Cortex	R/L	-32 24 -6

Note. The coordinates for each ROI, and which rs-network the given regions is considered a part of. MNI = Montreal Neurological Institute; R = right scanning direction; L=left scanning direction.

Dynamic causal modelling. With csd-DCM, the time series of each ROI is extracted and converted to csd, based on the observed BOLD-signal. The csd is expressed in hertz (Hz), and refers to the correlation in the frequency distribution of the BOLD-signal between brain regions, which is a representation of effective connectivity. As csd is modelled as a function of the frequency distribution (representing the activity) in another region, the effective connectivity parameters indicate the causal interference a region makes on another region (Friston et al., 2014; Zeidman, Jafarian, Corbin, et al., 2019).

The connectivity strength between regions must have a set prior value. These *priors* are not affecting the effective connectivity in any major way, other than preventing extreme values in the output (*posteriors*) (Friston et al., 2014; Zeidman, Jafarian, Corbin, et al., 2019). In this study, the *priors* were turned on for connections between all the included regions within DMN, CEN and SN. The csd-DCMs were specified for each rs-fMRI acquisition; as each subject underwent two rs-fMRI acquisitions, a total of 1188 acquisitions were included in the analysis. The result of the csd-DCM are parameters of effective connectivity between and within each region (A-matrix) and hemodynamic parameters (*transit time* for each region, *epsilon* and *deacy*). In addition, csd-values (α- and β-values) and Free Energy parameters are extracted (Friston et al., 2014; Zeidman, Jafarian, Corbin, et al., 2019).

The hemodynamic parameters are essentially descriptions of the Balloon Model; the *transit time* for each predefined region, *decay* as the global parameter of the BOLD-signal, and *epsilon* as the neuronal efficacy (Friston et al., 2000). DCM calculates *transit time* by dividing the resting venous CBV by the resting CBF, providing a measure of the dynamics of the BOLD-signal. With an increase in mean *transit time*, the BOLD-signal dynamics would be prolonged, but the amplitude would remain the same. *Epsilon* describes the relationship between CBF and neuronal activity; it reflects an increase in rCBF, which is expressed as a number of transients per second (Friston et al., 2000; Zeidman, Jafarian, Corbin, et al., 2019). *Decay* represents the

reduction of the BOLD-signal, which can suppress the post-stimulus undershoot if elevated sufficiently. *Decay*, or specifically the rate of *decay,* is related to the relaxation of smooth musculature of the arterioles.

In addition to hemodynamic and effective connectivity parameters, the spectral density values are extracted when using csd-DCM. These are expressed as α- and β-values, and reflect the amplitudes and exponents of the spectral density of the neuronal fluctuations, respectively. Further, model evidence, expressed as "Free Energy" is calculated. If the model evidence increases by including variables in the model, it is indicating that more of the model is explained when the given variables are included (Friston et al., 2014).

Between-Subject Variance

To test the hypotheses of between-subject variation in the parameters produced by the DCM, a hierarchical linear regression and a non-parametric test of between group variance (Kruskal-Wallis H Test) was conducted. The hierarchical linear regression was chosen as most of the independent variables were within a normal range, and therefore it was not viewed as beneficial to split the variables into groups. The BMI variable was however viewed as beneficial to split into groups. The groups were compared with Kruskal-Wallis H test. The continuous BMI variable was also included in the regression analysis.

Descriptive analyses. To make sure that the study sample represented the total HCP sample, in terms of BP, HCT, BMI and HbA1c, the distribution of these variables was examined. A two-tailed Pearson correlation analysis was conducted on the independent variables to investigate the relationship between them. In addition, the general descriptive statistics for the independent and dependent variables were examined.

Hierarchical linear regression analysis. Before the regression analysis was carried out, preliminary analysis in the form of a two-tailed Pearson correlation analysis was conducted

on the independent and dependent variables, to investigate the relationship between them. In addition, the assumptions of linear regression, namely the assumptions of a relatively large sample size, few extreme outliers, normality, linearity, multicollinearity and homoscedasticity was checked: Extreme outliers, defined as >3.0 interquartile from the mean, and outliers over the critical value as indicated by Mahalanobis' Distance, were removed. The data did not show multicollinearity (see Appendix E for the full correlation matrix for the independent variables). There were no major deviations from normality or linearity; indicating that these assumptions were met for most of the regression models. The effective connectivity parameters LIPC to ACC, PPC to mPFC and RIPC did not meet the assumptions and were therefore not included in the final regression analysis.

A hierarchical linear regression analysis was conducted on the independent variables (BP, HCT, BMI and HbA1c) and the dependent variables (DCM parameters) that showed a significant correlation (Two-tailed $p < .05$). If more than one independent variable correlated significantly with the same dependent variable, both were added to the same regression model. The effect of gender was controlled for, as it has been found to affect the activity in rs-networks, and as the normal range of HCT is known for being higher in men than in females.

It was examined whether the variance in the dependent variables could be significantly better predicted by the independent variables than gender alone. For the full models (including the independent variable(s) and gender) it was examined which of the variables that made a significant unique contribution to explaining the variance in the dependent variable, and whether the full model significantly predicted the dependent variable. To investigate the relative contribution of each factor independently, the standardized coefficient Standardized Beta of the coefficients t-test were examined, as well as R^2 Change for the F-test of the full models. The alpha value was set to 0.05, and the confidence interval was set to 95%.

Between group analysis of variance. The BMI variable was split into three groups for comparison. BMI is not normally distributed, therefore a non-parametric alternative for analysis of group variance, the Kruskal-Wallis H Test, was used to determine whether there were significant differences between the BMI groups on the DCM parameters. The test was carried out after the assumptions of the test was checked. The χ^2-distribution was defined by the *degrees of freedom* (K-1); in this case 2, as 3 groups were being compared.

In the cases of significant group differences, a pairwise comparison with Bonferroni corrections was used to investigate which groups significantly differed ($p < .05$). The Mean Rank Value was used to determine which of the groups showed a higher rank order, and effect sizes were calculated ($r = z/\sqrt{n+n}$).

Results

Within-Subject Estimates

Dynamic Causal Modelling. After the times series for each ROI were extracted, the csd-DCM provided the within-subject estimate of the effective connectivity between and within the regions of DMN, CEN and SN (A-matrix), the hemodynamic response parameters (*transit time*, *epsilon* and *decay*), the csd parameters of the neural fluctuations (α- and β-values), in addition to Free Energy (model evidence). The following analysis included these parameters as dependent variables.

Descriptive Statistics

The study sample was similar to the total HCP sample in terms of BP, HCT, BMI and HbA1c, in addition to similar distribution of gender and age; full sample (N = 1206; female =

656, male = 550, mean age = 28,8; SD = 3.6), study sample (N = 594, female = 310, male = 284, mean age = 28.8; SD = 3.6). See Table 3 for the distribution.

Table 3

Study Sample Compared to Full HCP Sample

Variable	Total HCP Sample (N = 1206)		Study Sample (N = 594)	
	Mean	SD	Mean	SD
BP				
Systolic	124	14.9	124.1	13.8
Diastolic	77	11.0	76.9	10.5
HCT	**43**	**4.7**	**44**	**4.9**
Female	41	4.2	41	4.7
Male	46	3.9	46	3.6
BMI	**27**	**5.9**	**26**	**5.1**
Female	27	6.5	26	5.8
Male	27	5.0	27	4.2
HbA1c	**5**	**0.4**	**5**	**0.4**

Note. The mean distribution of the biological variables in the total HCP sample, compared to the study sample, with SD; mean for each gender for HCT and BMI. SD = standard deviation; HCP = Human Connectome Project; BP = blood pressure; HCT = hematocrit; BMI = Body Mass Index; HbA1c = glycated hemoglobin.

Table 4

Descriptive Statistics for the Independent Variables

				Mean			Skewness		Kurtosis	
Variable	N	Min.	Max.	Statistic	Std. Error	SD	Statistic	Std. Error	Statistic	Std. Error
Sys BP	590	88	176	124.1	.569	13.8	.317	.101	.156	.201
Dia BP	590	40	113	76.9	.431	10.4	.199	.101	.321	.201
HCT	547	18	59	43.6	.210	4.9	-.916	.104	3.6	.209
BMI	593	16	45	26.2	.209	5.0	.978	.100	.844	.200
HbA1c	417	1.3	6.3	5.2	.018	.3	-3.2	.120	30.6	.238

Note: Descriptive statistics for the independent variables. Sys BP = systolic blood pressure; Dia BP = diastolic blood pressure; HCT = hematocrit; BMI = Body Mass Index; HbA1c = glycated hemoglobin; N = number of subjects; Min. = minimum score; Max. = maximum score; std. Error = standard error; SD = standard deviation.

The general descriptive statistics of the independent and dependent variables were examined, see Table 4. It revealed that there were missing scores on all of the independent variables, with HbA1c missing the most values (missing values = 177). For the BP variables there were subjects in the dataset with a systolic BP above 140mm Hg, which is categorized as hypertensive stage 2 if combined with a diastolic BP above 90mm Hg, which someone in the sample also had (see Table 1). The mean for the subjects were slightly elevated for systolic BP (above 120 mm Hg). The mean diastolic BP was within a normal range (less than 80mm Hg).

For the mean HCT score for each gender, see Table 3. These scores are categorized as being within the normal range for the population for each gender. The mean of the BMI variable was above 25, indicating that the mean of the study sample is categorized as overweight. For HbA1c there were some subjects with a below normal, and some with an above normal, score. However, with a high kurtosis, and low standard deviation, most of the scores are likely to be close to the mean; see Table 4. For the descriptive statistics of the dependent variables (DCM parameters), see Appendix E.

Correlations between the independent variables. The Pearson correlation analysis including the independent variables (confidence interval = 95%) revealed a significant relationship ($p < .05$) between systolic BP and HCT ($r = .105$, $p = .015$) and systolic BP and BMI ($r = .335$, $p = .000$). There was also a significant relationship between diastolic BP and HCT ($r = .085$, $p = .048$) and diastolic BP and BMI ($r = .291$, $p = .000$). Systolic and diastolic BP had the strongest significant covariation ($r = .680$, $p = .000$). The results confirmed some of the hypotheses on the relationship between the independent variables; H_8, H_9, H_{10}, and H_{12}. However, H_{11}, H_{13} and H_{14} were not confirmed. See Appendix F for the full correlation matrix.

Hierarchical Linear Regression

The Pearson correlation analyses between the independent and dependent variables conducted prior to the regression analyses (confidence interval = 95%) showed that there was a significant relationship between some of the variables ($p < .05$). The variables that did not show a significant correlation were not included in the regression models, as they were considered as not having a relationship between them that it would be useful to investigate further.

See Table 5 for the significant correlations between the independent variables and the hemodynamic parameters and Table 6 for the significant correlations for the effective connectivity parameters. For the csd parameters, the α-value was significantly correlated with diastolic BP ($r = .100$, $p = .015$), and the β-value was significantly correlated with diastolic BP ($r = -.087$, $p = .035$) and BMI ($r = -.091$, $p = .027$). Free Energy was significantly correlated with all the independent variables; diastolic BP ($r = .136$, $p = .001$), systolic BP ($r = .108$, $p = .009$), HCT ($r = -.155$, $p = .000$), BMI ($r = .150$, $p = .000$) and HbA1c ($r = .150$, $p = .002$). As can be seen from the correlation coefficients, and the ones in table 5 and 6, all of the significant

correlations are quite small; around r = .10 (Cohen, 1988, pp. 79-88). The rest of the independent and dependent variables were not significantly correlated.

Table 5

Significant Correlations Between the Independent Variables and the Hemodynamic Parameters

Independent Variable(s)	Hemodynamic Parameter	Pearson's r	Sig.
Sys BP	RIPC *transit time*	-.086	.011*
	Epsilon	.096	.020*
Dia BP	mPFC *transit time*	-.080	.050*
	LIPC *transit time*	-.090	.029*
	AI *transit time*	-.103	.012*
	DLPFC *transit time*	.082	.048*
	PPC *transit time*	.099	.016*
	Decay	.086	.036*
	Epsilon	.132	.001**
BMI	mPFC *transit time*	.120	.003**
	PCC *transit time*	-.081	.049*

Note. The table shows only the significant correlations between the independent variables and the hemodynamic parameters. Confidence interval = 95%. mPFC = medial prefrontal cortex; PCC = posterior cingulate cortex; LIPC/RIPC = left/right inferior cingulate cortex; AI = anterior insula; DLPFC = dorsolateral prefrontal cortex; PPC = posterior parietal cortex; Sys BP = systolic blood pressure; dia BP = diastolic BP; BMI = Body Mass Index. *$p < .05$, ** $p < .01$.

Table 6

Significant Correlations Between the Independent Variables and the Effective Connectivity Parameters

Independent Variable(s)	Effective Connectivity	Pearson's r	Sig.
Sys BP	PCC to mPFC	.091	.027*
	PCC to AI	-.081	.048*
	LIPC to PCC	-.100	.016*
	RIPC	.099	.017*
	RIPC to mPFC	-.118	.004**
	RIPC to ACC	-.113	.006**
	AI to ACC	-.082	.046*
	AI to DLPFC	-.114	.006**
	AI to PPC	-.125	.002**
	ACC to RIPC	.104	.011*
Dia BP	PCC to AI	-.105	.049*
	mPFC	.111	.007**
	LIPC to PCC	.086	.036*
	RIPC to ACC	-.087	.035*
	RIPC to PPC	-.094	.023*
	AI to ACC	-.113	.006**
	AI to DLPFC	-.094	.023*
	AI to PPC	-.156	.000**
	DLPFC to AI	.096	.019*
HCT	LIPC to RIPC	-.105	.014**
	LIPC to ACC	-.103	.016**
	PPC to mPFC	-.089	.037*
BMI	mPFC to to PCC	.085	.039*
	mPFC to RIPC	.085	.038*
	mPFC to AI	.085	.038*
	mPFC to ACC	.085	.039*
	AI to PCC	-.096	.019*
	ACC to PPC	.084	.040*
	PCC to AI	-.101	.049*
HbA1c	PCC to PPC	.124	.011*
	AI to PPC	-.121	.014*
	ACC to PPC	.110	.024*

Note. The table shows only the significant correlations between the independent variables and the effective connectivity parameters. Confidence interval = 95%. mPFC = medial prefrontal cortex; PCC = posterior cingulate cortex; LIPC/RIPC = left/right inferior cingulate cortex; AI = anterior insula; DLPFC = dorsolateral prefrontal cortex; PPC = posterior parietal cortex; ACC = anterior cingulate cortex; Sys BP = systolic blood pressure; dia BP = diastolic BP; BMI = Body Mass Index.

*$p < .05$, ** $p < .01$.

Hemodynamic parameters. For the result of the regression analysis with the hemodynamic parameters as outcome variables, see table 7. Gender alone significantly predicted RIPC *transit time*. Systolic BP made a significant contribution to this model, even though neither gender nor systolic BP made significant unique contributions. The full model did however significantly explain 1.3% of the variance.

Adding diastolic BP to the model did not explain significantly more of the variance in PPC *transit time* than gender alone, and the variable did not make a significant unique contribution, even though the full model was significant. Neither gender alone or the full models significantly predicted the variance in LIPC *transit time* and DLPFC *transit time*.

For PCC *transit time*, BMI made a significant contribution to the model, but the full model was not significant. For mPFC *transit time*, adding BMI and diastolic BP explained significantly more of the variance, both variables made significant unique contributions to the model, and the full model was significant; diastolic BP and BMI together explained 2.8% of the variance. For AI *transit time*, adding diastolic BP to the model made a significant contribution to explaining the variance, the variable made a significant unique contribution, and the full model was significant; diastolic explained 1.3% of the variance.

Table 7

Regression Table for Transit Time

		Modell Summary					Coefficients	
Transit Time	Model	R^2	R^2 Change	(df reg, df res) = F	Sig.	Sig. F Change	*beta*	Sig.
PCC	Gender	.001		(1, 579) = .479	.489			
	Gender	.010	.009	(2, 578) = 2.936	.054	.021	.035	.396
	BMI						-.096	.021*
mPFC	Gender	.000		(1, 575) = .198	.657			
	Gender	.028	.028	(3, 573) = 5.567	.001	.000	.028	.497
	Dia				**		-.130	.003**
	BP						.157	.000**
	BMI							
LIPC	Gender	.000		(1, 576) = .062	.804			
	Gender	.006	.006	(2, 575) = 1.803	.166	.060	.002	.961
	Dia BP						-.079	.060
RIPC	Gender	.008		(1, 576) = 4.509	.034			
	Gender	.013	.005	(2, 575) = 3.707	.025	.034	-.065	.133
	Sys BP						-.074	.090
AI	Gender	.000		(1, 576) = .479	.669			
	Gender	.013	.013	(2, 575) = 2.936	.020	.006	.036	.391
	Dia BP				*		-.116	.006**
DLPFC	Gender	.002		(1, 576) = 2.366	.125			
	Gender	.006	.005	(2, 575) = 2.679	.069	.085	.053	.211
	Dia BP						.073	.085
PPC	Gender	.004		(1, 576) = 2.432	.119			
	Gender	.010	.006	(2, 575) = 3.013	.050	.059	.052	.213
	Dia BP						.080	.059

Note. The results of the hierarchical linear regression analyses for the hemodynamic parameter *transit time,* for each region. The regression analysis with gender as predictor alone can be seen in the first row of each parameter, the full model including the independent variables can be seen in the second row. Confidence interval = 95%. mPFC = medial prefrontal cortex; PCC = posterior cingulate cortex; LIPC/RIPC = left/right inferior cingulate cortex; AI = anterior insula; DLPFC = dorsolateral prefrontal cortex; PPC = posterior parietal cortex; Sys BP = systolic blood pressure; Dia BP = diastolic BP; BMI = Body Mass Index; df reg = *degrees of freedom* regression; df res = *degrees of freedom* residual; *beta*= standardized coefficient beta. *$p < .05$, ** $p < .01$.

For the remaining hemodynamic parameters, namely *decay* and *epsilon*, gender did not significantly predict the variance alone. Diastolic BP made a significant unique contribution to explaining the variance in *decay*, but the full model was not significant. Diastolic BP and systolic BP made a significant contribution to the model, where diastolic BP made a significant unique contribution to explaining the variance in *epsilon*. The full model was significant; explaining 1.7% of the variance. See Table 8 for the regression table for these parameters.

Table 8

Regression Table for Decay and Epsilon

	Modell Summary						Coefficients	
	Model	R^2	R^2 Change	(df reg, df res) = F	Sig.	Sig. F Change	*beta*	Sig.
Decay	Gender	.001		(1, 576) = .532	.446			
	Gender	.009	.008	(2, 575) = 2.683	.069	.028	-.045	.286
	Dia BP						.092	.028*
Epsilon	Gender	.000		(1, 576) = .053	.813			
	Gender	.017	.017	(2, 575) = 3.400	.018*	.007	-.014	.749
	Dia BP						.123	.034*
	Sys BP						.015	.804

Note. The results of the hierarchical linear regression analyses for the hemodynamic parameters *decay* and *epsilon.* The regression analysis with gender as predictor alone can be seen in the first row of each parameter, the full model including the independent variables can be seen in the second row. Confidence interval = 95%. Sys BP = systolic blood pressure; Dia BP = diastolic BP; df reg = *degrees of freedom* regression; df res = *degrees of freedom* residual; *beta*= standardized coefficient beta.

*$p < .05$, ** $p < .01$.

Effective connectivity parameters. The regressions with effective connectivity parameters as outcome variables revealed that some of the independent variables contributed significantly to explaining more of the variance in the given parameter than gender, and that one or more of the independent variables contributed significantly to this tendency, with the full model (including gender) being significant ($p = < .05$). See Table 9 for these cases. The regressions were this was not the case are described below, and the full regression tables can be found in Appendix G; with *p* for the models including only gender, as well as for the full models and which variables are included in the given regression, *Sig. F Change* for each full model, and the Standardized Coefficient *beta* and *p* for the unique contribution of each independent variable.

Gender alone significantly explained variance in PCC to AI, mPFC to AI and LIPC to PCC, but the independent variables in the full models did not make a significant contribution to explaining the variance of the connections. Gender alone also significantly explained variance in RIPC to ACC, were systolic and diastolic BP made a significant contribution to the full model. Even though none of the variables made a unique significant contribution, the full model was significant. See Appendix G.1 for the full regression table.

Systolic BP made a significant contribution to explaining the variance in PCC to mPFC, but the full model did not reach statistical significance. BMI made a significantly unique contribution to explaining the variance in mPFC to RIPC and mPFC to ACC, but the full models did not reach statistical significance: mPFC to RIPC. Diastolic BP made a significant contribution to explaining the variance in RIPC to PPC and DLPFC to AI, but the full models did not reach statistical significance. BMI and HbA1c did not significantly contribute to explaining the variance in ACC to PPC, and the full model was not significant. See Appendix G.2 for the full regression table.

Systolic and diastolic BP made a significant contribution to explaining the variance in AI to ACC, but neither variable made a unique significant contribution. Still, the full model was significant. Diastolic and Systolic BP made a significant contribution to explaining the variance in AI to DLPFC, but neither variable made a unique significant contribution. Still, the full model was significant. Gender made a unique significant contribution to the full model, in explaining the variance in AI to PPC. Even though diastolic BP, systolic BP, BMI and HbA1c did not make significant unique contributions to the model, they jointly contribute significantly to explaining more of the variance in AI to PPC than gender alone. The full model was significant. See Appendix G.3 for the full regression table.

For the following regressions the independent variables made significant contributions to the models, and the full models were significant, with one or more of the variables making a unique significant contribution to the model. For more information, see Table 9. HbA1c made a significant contribution to explaining the variance in PCC to PPC, explaining 1.0% of the variance. Diastolic BP significantly contributed to explain the variance in mPFC, and significantly explaining 1.6% of the variance. BMI made a significant contribution to explaining the variance in mPFC to PCC, explaining 1.1% of the variance. HCT made a significant contribution to explaining the variance in LIPC to RIPC, explaining 1.2% of the variance. Systolic BP made a significant contribution to explaining the variance in ACC to RIPC, explaining 1.2% of the variance. Systolic BP made a significant contribution to explaining the variance in RIPC to mPFC, and the full model was significant and systolic BP accounted for 1.1% of the explained variance.

Table 9

Regression Table for Effective Connectivity Parameters

	Modell Summary						Coefficients	
Connections	Model	R^2	R^2 Change	(df reg, df res) = F	Sig.	Sig. F Change	*beta*	Sig.
PCC to PPC	Gender	.007		(1,410) = 2.790	.096			
	Gender HbA1c	.016	.010	(2,409) = 3.393	.035*	.047	-.077 .098	119 .047*
mPFC	Gender	.001		(1,575) = .343	.558			
	Gender Dia BP	.017	.016	(2,572) = 4.989	.007**	.002	-.045 .130	.285 .002**
mPFC to PCC	Gender	.000		(1,579) = .027	.870			
	Gender BMI	.011	.011	(2,578) = 3.150	.044*	.013	-.014 .104	.739 .013*
LIPC to RIPC	Gender	.001		(1,534) = .776	.379			
	Gender HCT	.013	.012	(2,533) = 3.514	.030*	.013	.031 -.128	547 .013*
ACC to RIPC	Gender	.001		(1,576) = .645	.422			
	Gender Sys BP	.013	.012	(2,575) = 3.745	.024*	.009	-.001 .114	.974 .009**
RIPC to mPFC	Gender	.008		(1,576) = 4.802	.029			
	Gender Sys BP	.019	.011	(2,575) = 5.648	.004**	.004	-.057 -.110	.188 .011*

Note. The results of the hierarchical linear regression analyses for the effective connectivity parameters were the full models contributed significantly to predicting the outcome variable, with the independent variables making a unique significant contribution to explaining the variance. The regression analysis with gender as predictor alone can be seen in the first row of each parameter, the full model including the independent variables can be seen in the second row. Confidence interval = 95%. mPFC = medial prefrontal cortex; PCC = posterior cingulate cortex; LIPC/RIPC = left/right inferior cingulate cortex; PPC = posterior parietal cortex; Sys BP = systolic blood pressure; Dia BP = diastolic BP; HCT = hematocrit; BMI = Body Mass Index; HbA1c = glycated hemoglobin; df reg = *degrees of freedom* regression; df res = *degrees of freedom* residual; *beta*= standardized coefficient beta.

*$p < .05$, ** $p < .01$.

Cross spectral density parameters. For the α- and β-values, gender alone did not significantly explain the variance of the dependent variables. Diastolic BP made a significant contribution to explaining the variance in the α-value, explaining 1.1% of the variance. Diastolic BP made a unique significant contribution to explaining the variance in the β-value, and the full model significantly better predicted the parameter than gender alone. However, the full model, including diastolic BP and BMI did not reach statistical significance. See Table 10 for more information.

Table 10

Regression Table for csd-Values

	Modell Summary						Coefficients	
csd-Parameter	Model	R^2	R^2 Change	(df reg, df res) = F	Sig.	Sig. F Change	*beta*	Sig.
Alpha (α)	Gender	.002		(1, 576) = 1.205	.273			
	Gender	.013	.011	(2,575) = 3.759	.024*	.012	-.062	.139
	Dia BP						.105	.012*
Beta (β)	Gender	.002		(1, 575) = 1.203	.273			
	Gender	.013	.011	(3, 573) = 2.498	.059	.044	-.062	.139
	[a] Dia BP						.105	.019*
	BMI						.002	.963

Note. The results of the hierarchical linear regression analyses for the csd values. The regression analysis with gender as predictor alone can be seen in the first row of each parameter, the full model including the independent variables can be seen in the second row. Confidence Interval = 95%. Dia BP = diastolic BP; BMI = Body Mass Index; df reg = *degrees of freedom* regression; df res = *degrees of freedom* residual; beta = standardized coefficient beta.

*$p < .05$, ** $p < .01$.

[a] Diastolic BP made a significant unique contribution to the model, and the full model was close to statistically significant.

Free energy. For the free energy parameter, the full model explained significantly more than gender alone. However, gender made the only significantly unique contribution to the full model. The full model explains around 7.9% of the variance in Free Energy, and BP, HCT, BMI and HbA1c accounted for 5.0% of the explained variance (see Table 10).

Table 10

Regression Table for Free Energy

	Modell Summary						Coefficients	
	Model	R^2	R^2 Change	(df reg, df res) = F	Sig.	Sig. F Change	*beta*	Sig.
Free Energy	Gender	.029		(1,405) = 12.063	.001			
	Gender	.079	.050	(6,400) = 5.750	.001**	.001	-.162	.007**
	Dia BP						.104	.124
	Sys BP						.053	.457
	BMI						.096	.068
	HCT						-.081	.157
	HbA1c						.060	.217

Note. The results of the hierarchical linear regression analyses for the free energy parameter. The regression analysis with gender as predictor alone can be seen in the first row, the full model including the independent variables can be seen in the second row. Confidence interval = 95%. Sys BP = systolic blood pressure; Dia BP = diastolic BP; HCT = hematocrit; BMI = Body Mass Index; HbA1c = glycated hemoglobin; df reg = *degrees of freedom* regression; df res = *degrees of freedom* residual; beta = standardized coefficient beta.

*$p < .05$, ** $p < .01$.

Put together, the results of the hierarchical linear regressions imply that the variance in the hemodynamic parameters mPFC *transit time*, AI *transit time* and *epsilon* can be predicted by diastolic BP for all the variables, and by BMI for mPFC transit time. These predictors significantly contributed to explaining more of the variance than gender alone, each made a significantly unique contribution to explaining the variance, and the full model was significant. In addition, diastolic BP made significant contribution to explaining the variance in the csd parameter α-value, indicating a positive relationship between diastolic BP and the α-value. The direction of the relationship between these hemodynamic parameters and diastolic BP and BMI indicates a weakening of the BOLD-signal; confirming H_1 and H_3. H_2 and H_4 was not confirmed, as the correlation analysis indicated little covariance between HCT and HbA1c with the hemodynamic parameters, and therefore no hierarchical linear regression analysis was conducted with these parameters as the outcome variables.

The independent variables that significantly predicted variance in the effective connectivity parameters were diastolic BP for mPFC, systolic BP for RIPC to mPFC and ACC to RIPC, HCT for LIPC to RIPC, BMI for mPFC to PCC and HbA1c for PCC to PPC; giving support to hypothesis H_5, H_6, and H_7.

The results indicate that gender seems to have a very small effect on the hemodynamic parameters, except for significantly explaining 0.8% of the variance in RIPC *transit* time. Gender significantly predicted variance in the effective connectivity parameters PCC to AI, mPFC to AI, LIPC to PCC, RIPC to mPFC and RIPC to ACC.

Analysis of Between Group Differences

The BMI variable was split into three groups; normal weight (19-24 kg., n = 262), overweight (25-29 kg., n = 202) and obese (>30 kg., n = 117), for comparison. See Appendix H for the frequency distribution of the groups across the BMI scores.

The assumptions of the Kruskal-Wallis H test were checked and met. For this dataset the dependent variables did not show a similar shape across groups and was therefore considered more useful to report mean rank values for comparison between groups, instead of medians.

Hemodynamic parameters. The only hemodynamic parameter that differed between groups was PCC *transit time* (normal weight $n = 262$, overweight $n = 202$, obese $n = 117$), χ^2 ($df = 2$, $n = 581$) = 8.718, $p = .013$. After the pairwise comparison with Bonferroni corrections, the significant difference between the groups were found to be between the overweight and the obese group, with the overweight group having a higher mean rank value (*mean* rank = 314.00) than the obese group (*mean rank* = 258), $p = .009$, $r = 0.166$. See Appendix I for all the Kruskal-Wallis H tests with the hemodynamic parameters.

Effective connectivity parameters. The Kruskal-Wallis H Test revealed some significant BMI group differences, which can be seen in Table 11, and Figure 1. After the pairwise comparison with Bonferroni corrections, the overweight group and the obese group significantly differed in the effective connectivity from PCC to mPFC, from PCC to RIPC, and within RIPC, with the overweight group having the highest mean rank value. The normal weight group and the overweight group significantly differed on effective connectivity from LIPC to PCC, from LIPC to mPFC, from LIPC to RIPC, from AI to mPFC and within RIPC. The normal weight group had the highest mean rank value for all the connections except for from AI to mPFC, where the overweight group had the highest mean rank value. The normal weight and the obese group significantly differed in effective connectivity from PCC to DLPFC and from mPFC to RIPC. For PCC to DLPFC the normal weight group had the highest mean rank value, indicating stronger effective connectivity, whereas the obese group had a higher mean rank value from mPFC to RIPC. As can be seen from Table 11, the effect sizes are low for all the

significant different groups (Cohen, 1988). For the results of the non-significant Kruskal-Wallis H test for effective connectivity, see Appendix J.

Cross spectral density parameters. The Kruskal-Wallis H test revealed no significant group differences on the csd parameters α-value (normal weight $n = 262$, overweight $n = 202$, obese $n = 117$), χ^2 ($df = 2$, $n = 581$) = .439, $p = .803$, and ß-value (normal weight $n = 262$, overweight $n = 202$, obese $n = 117$), χ^2 ($df = 2$, $n = 581$) = 2.644, $p = .267$.

Free Energy. The Kruskal-Wallis H Test revealed a significant group differences between the BMI groups (normal weight $n = 262$, overweight $n = 202$, obese $n = 117$), χ^2 ($df = 2$, $n = 581$) = 18.725, $p = .000$. The pairwise comparison found the groups that significantly differed to be the normal weight group (*mean rank* = 262.14) and the obese group (*mean rank* = 341.28), with the obese group having the highest mean rank, (*std.stat* = 4.293) $r = -.220$, $p = .000$.

Put together, group differences between BMI groups were significant for the hemodynamic parameter PCC *transit time,* giving support to H_3. In addition, multiple connections, mostly within DMN and between DMN and the other networks, showed significant BMI group differences, which gives support to H_6.

Table 11

Sig. Kruskal-Wallis H Tests with Effective Connectivity Parameters, with sig. Group Differences

	Kruskal – Wallis		Pairwise Comparisons				
Connections	Sig.	Chi ^{2}	Pairwise Comparison	Std. Stat.	Adj.Sig	*r*	Mean Rank
PCC to mPFC	.011*	8.938	NW – OB	1.598	.330		NW: 289.84
			OW – OB	2.966	.009**	.166	OW: 316.00
			NW – OW	-1.648	.298		OB: 260.39
PCC to RIPC	.003**	11.594	NW – OB	2.164	.091		NW: 292.99
			OW – OB	3.405	.002**	.190	OW: 316.92
			NW – OW	-1.509	.394		OB: 253.09
RIPC	.002**	12.476	NW – OB	1.067	.857		NW: 281.88
			OW – OB	3.277	.003**	.183	OW: 323.64
			NW – OW	-2.632	.025*	-.122	OB: 262.21
PCC to DLPFC	.030*	7.042	NW – OB	2.566	.031*	.131	NW: 306.07
			OW – OB	2.155	.094		OW: 299.17
			NW – OW	.435	1.000		OB: 258.78
mPFC to RIPC	.032*	6.899	NW – OB	-2.610	.027*	.134	NW: 274.42
			OW – OB	-1.431	.457		OW: 295.70
			NW – OW	-1.341	.539		OB: 322.52
LIPC to PCC	.013*	8.637	NW – OB	1.601	.328		NW: 316.65
			OW – OB	-.883	1.000		OW: 270.58
			NW – OW	2.904	.004**	.134	OB: 287.13
LIPC to mPFC	.010**	9.290	NW – OB	.769	1.000		NW: 313.84
			OW – OB	-1.787	.222		OW: 266.16
			NW – OW	3.005	.008**	.139	OB: 299.65
LIPC	.040*	6.435	.	.	.		.
LIPC to RIPC	.041*	6.409	NW – OB	1.556	.359		NW: 313.85
			OW – OB	-.551	1.000		OW: 274.83
			NW – OW	2.460	.042*	.114	OB: 285.16
AI to mPFC	.009**	9.368	NW – OB	-1.596	.331		NW: 268.59
			OW – OB	1.000	.952		OW: 316.76
			NW – OW	-3.037	.007**	-.140	OB: 298.02

Note. Showing the significant Kruskal-Wallis H Test for between BMI group differences in the effective connectivity parameters, and the pairwise comparison statistics. Total N = 585, normal weight *n* = 262, overweight *n* = 202, obese *n* = 117. *Degrees of Freedom* = 2. Std. Stat. =Standardized test statistic. Adj.Sig = Adjusted alpha-value after Bonferroni Corrections *r* = effect size. Dash indicates no data obtained, as the pairwise comparison was not run. PCC = posterior cingulate cortex; mPFC = medial prefrontal cortex; LIPC/ RIPC = left / right inferior parietal cortex; AI = anterior insula; DLPFC = dorsolateral prefrontal cortex. *p = .05, ** p = .01.

Figure 1

Significant Differences between BMI-groups in Effective Connectivity Parameters

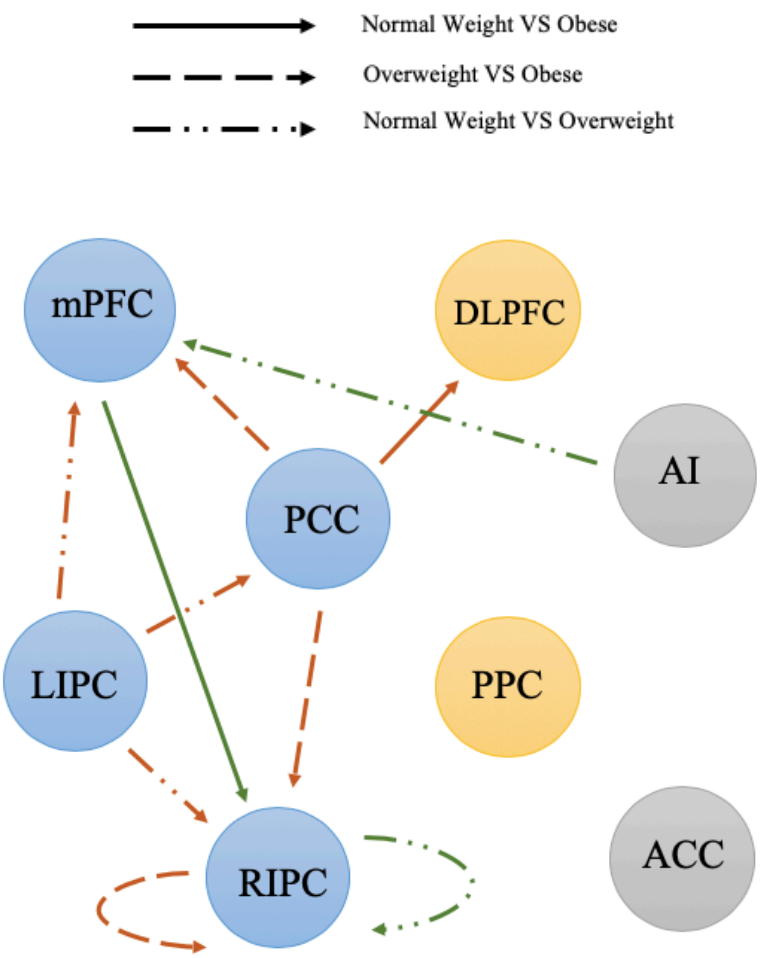

Note. The results of the significant group-differences of the Kruskal-Wallis H Test for the effective connectivity parameters. The arrows indicates which groups are being compared, and the directionality of the connection. Based on the mean rank value of the given groups in the comparison, it was determined whether the connection was strengthened (green arrow) or weakened (orange arrow) with increased BMI. The color of the circle indicates the network the given region is a part of; blue being DMN, yellow being CEN and grey being SN. As can be seen from the figure, all of the affected connections are within DMN, or between DMN and CEN or SN. mPFC = medial prefrontal cortex; LIPC/RIPC = left/right inferior parietal cortex; PCC = posterior cingulate cortex; DLPFC = dorsolateral prefronal cortex; PPC = posterior parietal cortex, AI = anterior insula; ACC = anterior cingulate cortex.

Discussion

Several of the primary hypotheses, regarding variability in hemodynamic and effective connectivity parameters, were supported. The results of the regression analyses imply that between-subject variance in the hemodynamic parameters of rs-fMRI is predicted by diastolic BP and BMI (confirming H_1) , and that variance in the effective connectivity within and between rs-networks is predicted by diastolic and systolic BP, HCT, BMI and HbA1c (confirming H_5, H_6 and H_7). The between-group comparison for BMI gives insight into hemodynamic and effective connectivity differences between BMI groups (confirming H_3 and H_6). As expected, the effect sizes were quite small, but as can be seen form the regression analysis with Free Energy, including the independent variables increases the explained model evidence; collectively explaining around 5 % of the variance. In addition, some of the secondary hypotheses, regarding the relationship among the independent variables were confirmed, namely H_8, H_9, H_{10}, and H_{12}.

Hemodynamic Parameters

Diastolic BP and BMI explained some of the variance in hemodynamic parameters, but the parameters did not seem to vary with HCT and HbA1c.

Blood pressure and body mass. Diastolic BP made a unique contribution to explaining the variance in the hemodynamic parameters *epsilon,* mPFC *transit time* and AI *transit time*, in addition to the csd α-value. *Epsilon* describes the relationship between CBF and neuronal activity, essentially reflecting an increase in rCBF; the number of evoked transients per second when the BOLD-signal is elicited. As diastolic BP showed a positive relationship with *epsilon*, higher diastolic BP is likely to increase the amplitude of the BOLD-signal response and undershoot; implying an increase in rCBF. As *epsilon* is a global measure, the relationship

between increased diastolic BP and increased BOLD-signal amplitude applies to all the brain regions included in this study.

Increased diastolic BP also had a negative effect on the *transit time* in mPFC and AI. *Transit time* predicts BOLD-signal dynamics by dividing CBV by CBF. A decrease in *transit time* indicates that the dynamics of the BOLD-signal is shortened, while the overall shape/amplitude of the BOLD-signal remains the same. As *epsilon* was positively related to diastolic BP in the current study, a change in the shape/amplitude of the BOLD-signal can be assumed as well. Taken together, an increase in diastolic BP increases the amplitude of the BOLD-signal globally, in addition to shortening it in the regions of mPFC and AI.

In addition, diastolic BP affected the csd-parameter α-value, exhibiting a positive relationship. The α-value reflects the amplitude of the spectral density of the neuronal fluctuations, which increase with increased diastolic BP. The relationship between increased BOLD-signal amplitude (*epsilon)* and increased α-value might reflect the same underlying mechanism of a more "intense" BOLD-signal. The variance in ß-value was also uniquely predicted by diastolic BP, explaining more of the variance than gender alone together with BMI, but the full model was only close to significant. This tendency might be a result of including both BMI and diastolic BP in the full model, and excluding BMI might have led the full model to being significant.

It was postulated in H_1 that increased BP would weaken the BOLD-signal, as the heightened pressure might represent increased segmental vascular resistance. The shortened *transit time* confirm this hypothesis for mPFC and AI, and the hemodynamic signal appear to be altered in all the regions of interest. The results indicate that diastolic BP affect the rate at which oHb is being utilized in the capillaries and dHb is transported to the veins; essentially weakening the response from the venous compartments in terms of the Balloon model proposed by Buxton et al. (1998). One explanation of this tendency might be related to stiffer venules

and veins, which could increase diastolic BP, and prevent the Balloon effect (Buxton, 2012; Buxton et al., 1998). The explanation of the observed variance is however probably multifaceted, as the dynamics of the BOLD-signal is complicated and generally poorly understood (Arthurs & Boniface, 2002; Ekstrom, 2010; Handwerker, Gonzalez-Castillo, D'esposito & Bandettini, 2012; Logothetis & Wandell, 2004). Exactly why diastolic BP was found to significantly predict variance in the hemodynamic parameters, and the same relationship was not found for systolic BP should be further explored in future studies.

In addition, increased BMI was found to positively affect mPFC *transit time*, in the regression analysis; essentially prolonging the BOLD-signal in this region, while the shape/amplitude remain the same. However, *transit time* in PCC was higher for the overweight group compared to the obese group, in the group comparison analysis; essentially reflecting a shortening of the BOLD-signal with increased BMI. Higher BMI is associated with decreased CBV, which is thought to alter the Balloon effect in terms of making the BOLD-signal shorter (Buxton et al., 1998; Lemmens et al., 2006). Therefore, the results from the group comparison analysis is more in line with the expected relationship between BMI and the BOLD-signal, in this case in the region of PCC. The results are somewhat unclear, as the group comparison gives support to H_3, while the regression analysis does not. It might however be the case that the hemodynamic response in brain regions are affected differently by increased BMI.

Global and regional coupling of cardiovascular and BOLD-signal fluctuations. The effect BMI and BP have on *transit time* is not evident in all the regions within the rs-networks, but are limited to mPFC and AI for diastolic BP, and mPFC and PCC for BMI. mPFC and AI are situated close to two of the big arteries of the brain, namely arteria cerebri anterior and media, which might be one explanation of why these regions appear to be sensitive to differences in hemodynamics. These results are highly intriguing as mPFC and AI are the main hubs of DMN and SN.

As mentioned, the low frequency fluctuations (LFFs) of the rs-fMRI BOLD-signal and the frequency of cardiovascular fluctuations are within the same range; below 0.10 Hz for the BOLD-signal and around 0.08 Hz for the cardiovascular LFFs (Zhu et al., 2015). The results of the current study are in line with previous results, finding the BOLD-signal to be highly coupled with cardiovascular fluctuations and CBF globally, and with regions within DMN showing the strongest significant coupling (Kobuch et al., 2019; Tak, Wang, Polimeni, Yan & Chen, 2014). The variability in diastolic BP and BMI might therefore have affected the BOLD-signal of previously conducted functional connectivity studies, which can have been interpreted as changes in connectivity, while actually being attributable to hemodynamic variability (Rangaprakash, Wu, Marinazzo, Hu & Deshpande, 2018).

In the current study, the variance that diastolic BP and BMI explain collectively is 2.8% in mPFC *transit time*, diastolic BP explain 1.3% of the variance in AI *transit time* and 1.7% for *epsilon.* When considering all of the endogenous and exogenous factors that have been found to affect connectivity of rs-networks and the BOLD-signal, these components might be contributing factors to the overall low replicability and variability in rs-fMRI studies, even as the amount of explained variance by diastolic BP and BMI is fairly low. The results for diastolic BP is also in line with previous research, as it is indicated that around 2.2 % of the variance in the BOLD-signal is explained by mean beat-to-beat BP (Whittaker et al., 2019).

Hematocrit and glycated hemoglobin. HCT and HbA1c did not significantly correlate with the hemodynamic parameters and were therefore not included in any of the regression analyses. As there was no relationship between HCT and the hemodynamic parameters, H_2 was not supported. The lack of correlation might be related to effective cerebral autoregulation; with increased HCT the arterioles of the brain contract, increasing the pressure, so the blood perfusion remains stable. The correlation between HCT and diastolic and systolic BP was significant, but fairly low in this study, which might be a result of fairly homogenous scores

within the normal range for HCT, in the current sample. However, the lack of correlation between HCT and the hemodynamic parameters is not in line with previous research from task-based fMRI, which have found HCT to affect BOLD-signal dynamics by increasing the BOLD-signal activation (Levin et al., 2001; Xu et al., 2018). The result of this study indicates that the relationship between BOLD-signal activation and HCT might be different in rs-fMRI.

HbA1c was included in this study as it has been found to be related to body fat (Iso et al., 1991), and therefore a similar relationship was hypothesized between the hemodynamic response and HbA1c as between hemodynamic response and BMI. Interestingly, in the current study HbA1c was not significantly correlated with BMI, nor any of the other endogenous factors. Similar to the HCT results, this might be related to relatively homogenous scores, with few subject having above normal scores. HbA1c was also not significantly correlated with the hemodynamic parameters and was therefore not included in the regression analyses. The lack of relationship goes against the postulated H_4, but larger variability on the scores might have affected the results. However, as the aim was to study healthy individuals, including a sample with more deviant scores was beyond the scope of the current study.

Effective Connectivity

Blood pressure. As no previous studies to my knowledge have indicated a relationship between normotensive BP and changes in connectivity, and as BP was assumed to mostly affect the hemodynamic parameters, no hypothesis was made on the relationship between BP and effective connectivity. Diastolic BP did however predict some of the variance in within-mPFC connectivity, displaying a positive relationship. The effective connectivity parameters produced by csd-DCM for one region alone, is referred to as the "self-inhibitory connection of" mPFC (Zeidman, Jafarian, Corbin, et al., 2019). The positive relationship with diastolic BP therefore indicates that mPFC is more inhibited with increased diastolic BP. Systolic BP predicted some

of the variance in effective connectivity from RIPC to mPFC, displaying a negative relationship, and a positive relationship from ACC to RIPC. The findings indicating a positive relationship between BP and connectivity might be related to previous research indicating altered connectivity with hypertension, which have been found to be related to cognitive impairment (Bu et al., 2018).

Body mass. In the regression analysis, increased BMI predicted a strengthening of the effective connectivity from mPFC to PCC, within DMN, which is not in line with H_6. The between-group analysis did however to a large extent confirm this hypothesis:

The overweight group had stronger effective connectivity in the connections PCC to mPFC, PCC to RIPC, and within RIPC (self-inhibitory connection), compared to the obese group which might indicate a weakening of the internal cohesiveness of DMN with increased BMI. The normal weight group had stronger effective connectivity in LIPC to PCC, LIPC to mPFC, LIPC to RIPC and within RIPC (self-inhibitory connection), compared to the overweight group. However, the overweight group had stronger connectivity from AI to mPFC, compared to the normal weight group. The results indicate an internal weakening of the connectivity within DMN with increased BMI, as well as stronger connectivity from SN to DMN. The normal weight group also had stronger effective connectivity in PCC to DLPFC, compared to the obese group, which indicates stronger effective connectivity from DMN to CEN with normal weight. The obese group showed stronger effective connectivity in mPFC to RIPC, compared to the normal weight group, which was the only connection within the DMN that was stronger with increased BMI, which does not support H_6.

These results are in line with the previously described research on changes in connectivity with increased BMI, and mostly support H_6. As suggested in those studies, the result might be reflecting poorly regulated eating behavior, as networks involved in balancing sensory-driven and internally guided behavior are affected (Doucet et al., 2017; Sadler et al.,

2018). The current study contribute to a deeper understanding of the interactions between these networks, as effective connectivity not functional connectivity is investigated. It is for example interesting to notice that the strengthened connection between AI and mPFC with increased BMI, namely between SN and DMN, is in fact a *from* SN *to* DMN. In addition, connections from LIPC to several regions with DMN appear to be weaker with increased BMI, which might indicate that LIPC mediates the weakened connectivity in the other regions; PCC, mPFC and RIPC. This speaks for the importance of implementing effective connectivity analyses in rs-fMRI studies to a larger degree, as the shortcomings of functional connectivity analyses might lead to false conclusions being drawn.

It should be mentioned that when merely examining the significant group differences, the relationship between BMI and effective connectivity, H_6 is to a large degree being supported and the results are fairly in line with previous studies. However, when taking the mean rank of all of the groups into consideration, a non-linear relationship appear between the groups for some of the effective connectivity parameters. This might be why the results differ somewhat from the regression analysis, as it assumes a linear relationship. It might also be why previous research has indicated a linear relationship between higher BMI and changes in rs-connectivity, as most of the studies compare only two groups (see Section "Endogenous Sources of BOLD-Signal and rs-Connectivity Variability"). This relationship could be further investigated in future studies.

Hematocrit. HCT displayed a negative relationship with the effective connectivity from LIPC to RIPC, essentially weakening the internal connectivity of DMN, which in part confirms H_5. However, previously mentioned studies have indicated that HCT account for a weakening of the internal cohesiveness of all of the rs-networks included in this study (Yang et al., 2015). As HCT was mostly not correlated with the effective connectivity parameters, or otherwise not met the assumptions of regression analysis, it was only possible to perform one regression

analysis, namely from LIPC to RIPC, with HCT as predictor. However, one might consider the correlation analysis as a result in itself, indicating that there is a minimal relationship between HCT and effective connectivity of rs-networks.

Glycated hemoglobin. HbA1c exhibited a positive relationship with the effective connectivity from PCC to PPC (from DMN to SN) which partly confirms H_7. A weakening of the internal connectivity in CEN and SN was however not observed. Especially, the results are not in line with previous research indicating altered connectivity in AI and its connections. Due to the lack of correlation between HbA1c and most of the effective connectivity parameters, the only regression analysis including HbA1c as predictor and a connection with AI as a region was AI to ACC, were HbA1c did not contribute to explaining the variance. Compared to similar studies on HbA1c and rs-network alterations, which often specifically focuses on subjects with pre-diabetes or diabetes, the current study included mostly normal scores, which might have contributed to the result (Liu et al., 2017; Sadler et al., 2019; Yang et al., 2016).

Seen together, the results indicate that all the included factors included in this study can affect the underlying connectivity of the resting human brain, and that diastolic BP and BMI specifically can affect the measured BOLD-signal. As the effect sizes and the percent of explained variance are low, these factors are likely to not cause a large degree of variability in the results independently. However, as implied by Free Energy, they might collectively contribute to unreliable results.

Limitations of the Current Study

Testing for between-subject effects. When it comes to the regression analysis conducted in this study, it should be noted that the correlation analyses preformed prior to the regression analyses implied that even for the significant correlations, the relationship between the variables were quite low (around .10), meaning they were not above .30, which is often

recommended for regression analysis. The results of these analyses might therefore be somewhat uncertain. The reason for the low correlations between the independent and dependent variables might be due to an actual absence of covariance, or it might be due to fairly homogenous scores on the independent variables.

In addition, the use of regression analysis might be criticized in general. Especially in terms of effective connectivity, as it is uncertain whether it is useful to discuss explained variance by the independent variables in the effective connectivity parameter; partly as the amount of variance they explain are fairly low, and as it is uncertain whether the variance would actually have an effect on the connectivity of the resting brain. However, using regression to examine percentage of explained variance in the hemodynamic parameters is probably more informative, as the results are in line with previous studies using different analyzing techniques (Whittaker et al., 2019).

However, the planned analysis for the hypotheses testing in this study was Parametric Empirical Bayes (PEB). These analyses were stopped due to occurring errors, that we were unable to solve partly as a consequence of the outbreak of the Covid-19 epidemic. There are some advantages of using PEB with DCM as compared to other GLMs, and it can therefore be considered a limitation of this study that a more traditional GLM was utilized for the analyses of between-subject effects on the DCM parameters. Specifically, many of the analyses were not performed with HCT and HbA1c, as the assumptions of the regression analysis prevented it. Using PEB instead would allow for all the scores on all the independent variables to be analyzed with the DCM parameters, to examine their effect.

Parametric Empirical Bayes. PEB is based on the principles of Bayesian statistics, and makes inferences about between-subject effects based on the csd-DCM. A hierarchical model would convey the estimated csd of the rs-fMRI timeseries and their uncertainty (covariance) from subject to group level. It enables hypotheses about similarities and differences across

subjects to be tested. First, within-subject effects design matrix specification would define which DCM connectivity parameters that could receive between-subject effects. Secondly, the PEB model can be inverted, which estimates the between-subject parameters (Zeidman, Jafarian, Seghier, et al., 2019). The model evidence for the models can then be used for hypothesis testing, by comparing the model evidence for reduced models with the full model; Bayesian model comparison. This involves comparing models with certain *priors* (combinations of parameters "switched" on or off) with the full model (all priors "switched" on). Comparing full and reduced models in this manner resembles performing a F-test in e.g. linear regression (Zeidman, Jafarian, Seghier, et al., 2019).

The PEB approach offer several benefits compared to the traditional statistical analyses used in this thesis. Firstly, PEB takes both the uncertainty of the estimated parameters from the first-level DCM, as well as the expected values, into consideration at group level. Other GLMs in contrast, bring merely the expected values to group level, leaving out the covariance. Therefore, PEB will in practice let more precise parameter estimates have greater influence on the between-subject results, as it down-weights the results from subjects with noisy or uncertain parameter estimates. Secondly, PEB is a hierarchical model with random effects on *parameters* rather than *models*. It makes the assumption that the difference between subjects lies in the strength of the connections within or between a network, while assuming e.g. the same underlying architecture for all subjects. As mentioned, this would have allowed the use of all the continuous variables, as well as group comparisons of BMI groups, while still controlling for factors like gender (Zeidman, Jafarian, Seghier, et al., 2019).

The variables provided by HCP. Using already existing data is arguably favorable in research. As this thesis is related to the replication crisis, and open access data bases are put forward in an attempt to combat some of the problems regarding the replication crisis, it seemed beneficial to use HCP data for this study. It is also justifiable from an ethical standpoint; if

existing data is available it should be used to minimize the potential stress experienced by the subjects that would otherwise take part in the study. There are however some limitations to the HCP data when it comes to answering the research question at hand. For example, the information provided by HCP on their research procedure has some shortcomings, especially related to the lack of information on *how* and *when* the data was collected. In addition, as the data is collected for anyone to use, it is not tailored to a specific study design, as it would be if the data was collected for a particular study.

How the data was collected. HCP does not provide information on what BP apparatus that was used; the variables available speaks for BP as measured with a conventional BP apparatus, which gives a score on the systolic and diastolic BP, measured in mm/Hg. It could however have been beneficial to use a beat-to-beat measurement of BP, as it provides more information of the subject's BP while lying in the MR-scanner. In addition, the beat-to-beat measure of BP can be compared to the LFFs of the BOLD-signal (Kobuch et al., 2019; Whittaker et al., 2019).

When the data was collected. In the current study it would be beneficial with precise information on exactly *when* the biological measures were collected, as some of the variables, like BP, are known to vary across the day. As rs-fMRI results have been shown to vary with time of day, following a circadian rhythm, it would be advantageous if information on when BP was measured was available, as the relationship between rs-fMRI variability, time of day and BP could be further explored (Hodkinson et al., 2014). However, HCP only provides a general outline of the data collection, and they state that the order might vary slightly, which contributes to potential confounders specific to this study. Further, some variables, like BP, are not listed in the full overview of the data collection, which can be seen in Appendix D (Van Essen et al., 2013).

General limitations. In addition to the limitations related to how and when the variables were collected, some of them also have some general issues related to them. For example BMI, which is a well-known and often used measure of body mass, has been criticized for not being sensitive enough to differences in built, which might lead to subjects with higher muscle mass being categorizes as overweight (Deurenberg, Yap, Wang, Lin & Schmidt, 1999). HCP also provides information on the weight of the subjects, but as BMI takes the height of the individual into consideration, it was viewed as more useful in the current study.

It should however also be mentioned that some of the participants were severely obese, and as the current study aimed at studying a sample from a healthy population, these subjects might be considered as not falling into that category. The same applies to the subjects with high scores on BP.

Further, the subjects in the current study are related to each other, namely being monozygotic and heterozygotic twins, in addition to their non-twin siblings. As monozygotic twins have the same DNA and often share the same environment, they might have fairly similar scores on all the independent variables as well as having similar underlying neuronal structure (Van Essen et al., 2012). It can be viewed as a potential limitation of this study if both twins from the same monozygotic twin pair are included as subjects in this study. It is arguably similar to having the data from one subject put into the analysis twice (Smith & Nichols, 2018). The distribution of sibling status (see Appendix K) show that, in the current study 178 (30%) of the subject were monozygotic twins. Therefore, half of these (15%) might have scores that confounds the dataset, if their respective monozygotic twin is also included in the sample, and if they in fact are identical to their monozygotic twin, in terms of their score on the endogenous factors and rs-connectivity. However, the csd-DCM analysis was performed with these subjects as the same sample was to be used in another study, and considering DCM analyzing time and

that a high number of subjects was aimed for, this sample was considered sufficient for this study as well. Future research should aim to control for this possible interfering factor.

Future Studies and Implications

The current study adds to the growing body of research on rs-fMRI variability. As the results indicated that some of the hemodynamic, effective connectivity and csd-parameters can be affected by BP, HCT, BMI and HbA1c, it might be advantageous for future studies to take these variables into account when studying rs-networks, to increase the studies reproducibility; in line with the overarching goal of the current study.

In addition, some of the benefits of using DCM are highlighted with the current study. To a larger degree utilizing the DCM technique would enable future studies to assess if their results arise from actual neuronal changes, or if the changes merely represent variation in cerebral hemodynamics. As mentioned, using PEB instead of traditional GLMs for between-subject analysis was planned for the current study, and a future follow-up study should be conducted with PEB to investigate whether the results remain the same.

To include subjects that have a wider range of scores on the independent variables could also be beneficial. However, the results of the current study support the notion that variability in the BOLD-signal and connectivity of rs-networks is to be found within a fairly healthy population. Repeated measures would give valuable insight into how much of the observed between-subject variation that can be attributed to within-subject variation. This was not within the scope of the current study, but could be implemented in future studies.

As the results of this study indicate that the included endogenous factors are associated with changes in the underlying connectivity *and* hemodynamic variability of rs-networks, it adds to the number of studies that undermine the notion of rs-networks as being stable between subjects in terms of connectivity, as well as being susceptible to hemodynamic variation caused

by BP and BMI. Interestingly, DMN seems to be the most inherently unstable of the rs-networks, as it is susceptive to vary with the endogenous factors in both hemodynamic and effective connectivity parameters. Seen together with results from other studies, the wide range of potential sources of variability might be one of the reasons why it has been proven a challenge to come to a unified view on the function of DMN. In addition, the results implicate that DMN might not inhabit the between-subject stability which it is ascribed when studying clinical deviations (Greicius et al., 2004; Mevel et al., 2011).

Conclusion

The low cost, short scanning times and absence of task, which initially made rs-fMRI an intriguing, useful and popular tool for neuroimaging, comes with a price. Evidently, the rs-networks are susceptible to a variety of exogenous and endogenous factors, which makes the results of the studies unreliable and as a consequence challenging to replicate. This tendency adds to the difficulty of studying and understanding the function of rs-networks like DMN and using alterations in rs-networks as a clinical marker of disease. Seen together with previous studies and results, the current study is an indicator of the nature of DMN as inheritably unstable, in which case it is unsurprising that its function seems to "slip through the fingers" of the researcher. If rs-networks are to be truly understood, studies should at least take the effect of blood pressure and BMI into account, to ensure more reliable results for the future. By doing so, researcher would also take a step in the right direction in terms of the ongoing replication crisis.

Referances

Agcaoglu, O., Miller, R., Mayer, A. R., Hugdahl, K. & Calhoun, V. D. (2015). Lateralization of resting state networks and relationship to age and gender. *NeuroImage, 104*(1), 310-325. doi:10.1016/j.neuroimage.2014.09.001

Alexis, O. (2009). Providing best practice in manual blood pressure measurement. *British Journal of Nursing, 18*(7), 410-415. doi:10.12968/bjon.2009.18.7.41654

Allen, E. A., Erhardt, E. B., Damaraju, E., Gruner, W., Segall, J. M., Silva, R. F., . . . Kalyanam, R. (2011). A baseline for the multivariate comparison of resting-state networks. *Frontiers in systems neuroscience, 5*, 1-23. doi:10.3389/fnsys.2011.00002

An, H., Rajeev, O., Huang, D., Yang, J., Li, J., Yu, F., . . . Zhu, W. (2015). Influence of internal carotid artery stenosis, blood pressure, glycated hemoglobin, and hemoglobin level on fMRI signals of stroke patients. *Neurological research, 37*(6), 502-509. doi:10.1179/1743132815Y.0000000004

Arthurs, O. J. & Boniface, S. (2002). How well do we understand the neural origins of the fMRI BOLD signal? *TRENDS in Neurosciences, 25*(1), 27-31.

Attinger, E. O. (1969). Wall properties of veins. *Transactions on Biomedical Engineering, 16*(4), 253-261. doi:10.1109/TBME.1969.4502657

Azevedo, F. A., Carvalho, L. R., Grinberg, L. T., Farfel, J. M., Ferretti, R. E., Leite, R. E., . . . Herculano-Houzel, S. (2009). Equal numbers of neuronal and nonneuronal cells make the human brain an isometrically scaled-up primate brain. *Journal of Comparative Neurology, 513*(5), 532-541. doi:10.1002/cne.21974.

Beckmann, C. F., DeLuca, M., Devlin, J. T. & Smith, S. M. (2005). Investigations into resting-state connectivity using independent component analysis. *Philosophical Transactions*

of the Royal Society B: Biological Sciences, 360(1457), 1001-1013. doi:10.1098/rstb.2005.1634

Beyer, F., Kharabian Masouleh, S., Huntenburg, J. M., Lampe, L., Luck, T., Riedel-Heller, S. G., . . . Villringer, A. (2017). Higher body mass index is associated with reduced posterior default mode connectivity in older adults. *Human brain mapping, 38*(7), 3502-3515. doi:10.1002/hbm.23605

Birn, R. M. (2012). The role of physiological noise in resting-state functional connectivity. *NeuroImage, 62*(2), 864-870. doi:10.1016/j.neuroimage.2012.01.016

Biswal, B. (2012). Resting state fMRI: a personal history. *NeuroImage, 62*(2), 938-944. doi:10.1016/j.neuroimage.2012.01.090

Biswal, B., Zerrin Yetkin, F., Haughton, V. M. & Hyde, J. S. (1995). Functional connectivity in the motor cortex of resting human brain using echo-planar MRI. *Magnetic resonance in medicine, 34*(4), 537-541. doi:10.1002/mrm.1910340409

Bredt, D. S., Hwang, P. M. & Snyder, S. H. (1990). Localization of nitric oxide synthase indicating a neural role for nitric oxide. *Nature, 347*(6295), 768-770. doi:10.1038/347768a0

Bressler, S. L. & Menon, V. (2010). Large-scale brain networks in cognition: emerging methods and principles. *Trends in cognitive sciences, 14*(6), 277-290. doi:10.1016/j.tics.2010.04.004

Bu, L., Huo, C., Xu, G., Liu, Y., Li, Z., Fan, Y. & Li, J. (2018). Alteration in brain functional and effective connectivity in subjects with hypertension. *Frontiers in physiology, 9*, 1-12. doi:doi: 10.3389/fphys.2018.00669

Bucholz, K. K., Cadoret, R., Cloninger, C. R., Dinwiddie, S. H., Hesselbrock, V., Nurnberger Jr, J., . . . Schuckit, M. A. (1994). A new, semi-structured psychiatric interview for use

in genetic linkage studies: a report on the reliability of the SSAGA. *Journal of studies on alcohol, 55*(2), 149-158. doi:10.15288/jsa.1994.55.149

Buckner, R. L., Andrews-Hanna, J. R. & Schacter, D. L. (2008). The brain's default network: anatomy, function, and relevance to disease. *1124*(1), 1-38. doi:10.1196/annals.1440.011

Buckner, R. L. & DiNicola, L. M. (2019). The brain's default network: updated anatomy, physiology and evolving insights. *Nature reviews neuroscience, 20*(1), 593-608. doi:10.1038/s41583-019-0212-7

Buckner, R. L. & Krienen, F. M. (2013). The evolution of distributed association networks in the human brain. *Trends in cognitive sciences, 17*(12), 648-665. doi:10.1016/j.tics.2013.09.017

Button, K. S., Ioannidis, J. P., Mokrysz, C., Nosek, B. A., Flint, J., Robinson, E. S. & Munafò, M. R. (2013). Power failure: why small sample size undermines the reliability of neuroscience. *Nature reviews neuroscience, 14*(5), 365-376. doi:10.1038/nrn3475

Buxton, R. B. (2012). Dynamic models of BOLD contrast. *NeuroImage, 62*(2), 953-961. doi:10.1016/j.neuroimage.2012.01.012

Buxton, R. B., Uludağ, K., Dubowitz, D. J. & Liu, T. T. (2004). Modeling the hemodynamic response to brain activation. *NeuroImage, 23*, 220-S233. doi:10.1016/j.neuroimage.2004.07.013

Buxton, R. B., Wong, E. C. & Frank, L. R. (1998). Dynamics of blood flow and oxygenation changes during brain activation: the balloon model. *Magnetic resonance in medicine, 39*(6), 855-864. doi:10.1002/mrm.1910390602

Calhoun, V. D., Adali, T., Pearlson, G. D. & Pekar, J. J. (2001). A method for making group inferences from functional MRI data using independent component analysis. *Human brain mapping, 14*(3), 140-151. doi:10.1002/hbm.1048

Chandalia, H. & Krishnaswamy, P. (2002). Glycated hemoglobin. *Current Science, 83*(12), 1522-1532.

Chao, S.-H., Liao, Y.-T., Chen, V. C.-H., Li, C.-J., McIntyre, R. S., Lee, Y. & Weng, J.-C. (2018). Correlation between brain circuit segregation and obesity. *Behavioural brain research, 337*(1), 218-227. doi:10.1016/j.bbr.2017.09.017

Choe, A. S., Jones, C. K., Joel, S. E., Muschelli, J., Belegu, V., Caffo, B. S., . . . Pekar, J. J. (2015). Reproducibility and temporal structure in weekly resting-state fMRI over a period of 3.5 years. *PloS one, 10*(10). doi:10.1371/journal.pone.0140134

Cipolla, M. J. (2009). *Control of cerebral blood flow*. San Rafael: CA, US: Morgan & Claypool Life Sciences. https://www.ncbi.nlm.nih.gov/books/NBK53082/

Clark, D. D. & Sokoloff, L. (1999). Circulation and energy metabolism of the brain. In G. J. Siegel, B. W. Agranoff, & R. W. Albers (Eds.), *Basic neurochemistry: Molecular, Cellular and Medical Aspects* (6 ed., Vol. 2, pp. 565-590). Philadelphia: Lippincott-Raven.

Cohen, J. W. (1988). *Statistical power analysis for the behavioral sciences* (2 ed.). Hillsdale, NJ: Lawrence Erlbaum Associates.

Collaboration, O. S. (2015). Estimating the reproducibility of psychological science. *Science, 349*(6251), 943-952. doi:10.1126/science.aac4716

Craig, A. D. (2009). How do you feel--now? The anterior insula and human awareness. *Nature reviews neuroscience, 10*(1), 59-70. doi:10.1038/nrn2555

Crottaz-Herbette, S. & Menon, V. (2006). Where and when the anterior cingulate cortex modulates attentional response: combined fMRI and ERP evidence. *Journal of cognitive neuroscience, 18*(5), 766-780. doi:10.1162/jocn.2006.18.5.766

Curtis, B. J., Williams, P. G., Jones, C. R. & Anderson, J. S. (2016). Sleep duration and resting fMRI functional connectivity: examination of short sleepers with and without perceived daytime dysfunction. *Brain and behavior, 6*(12). doi:10.1002/brb3.576

Deurenberg, P., Yap, M. D., Wang, J., Lin, F. & Schmidt, G. (1999). The impact of body build on the relationship between body mass index and percent body fat. *International Journal of Obesity, 23*(5), 537-542. doi:10.1038/sj.ijo.0800868

Doll, A., Sorg, C., Manoliu, A., Meng, C., Wöller, A., Förstl, H., . . . Riedl, V. (2013). Shifted intrinsic connectivity of central executive and salience network in borderline personality disorder. *Frontiers in human neuroscience, 7*, 1-13. doi:10.3389/fnhum.2013.00727

Doornweerd, S., van Duinkerken, E., de Geus, E. J., Arbab-Zadeh, P., Veltman, D. J. & IJzerman, R. G. (2017). Overweight is associated with lower resting state functional connectivity in females after eliminating genetic effects: a twin study. *Human brain mapping, 38*(10), 5069-5081. doi:10.1002/hbm.23715

Doucet, G. E., Rasgon, N., McEwen, B. S., Micali, N. & Frangou, S. (2017). Elevated body mass index is associated with increased integration and reduced cohesion of sensory-driven and internally guided resting-state functional brain networks. *Cerebral Cortex, 28*(3), 988-997. doi:10.1093/cercor/bhx008

Duncan, N. W. & Northoff, G. (2013). Overview of potential procedural and participant-related confounds for neuroimaging of the resting state. *Journal of psychiatry & neuroscience: JPN, 38*(2), 84-96. doi:10.1503/jpn.120059

Ekstrom, A. (2010). How and when the fMRI BOLD signal relates to underlying neural activity: the danger in dissociation. *Brain research reviews, 62*(2), 233-244. doi:10.1016/j.brainresrev.2009.12.004

Faraci, F. M. & Heistad, D. D. (1990). Regulation of large cerebral arteries and cerebral microvascular pressure. *Circulation research, 66*(1), 8-17. doi:10.1161/01.RES.66.1.8

Fox, M. D., Snyder, A. Z., Vincent, J. L., Corbetta, M., Van Essen, D. C. & Raichle, M. E. (2005). The human brain is intrinsically organized into dynamic, anticorrelated functional networks. *Proceedings of the National Academy of Sciences, 102*(27), 9673-9678. doi:10.1073/pnas.0504136102

Friston, K. J., Harrison, L. & Penny, W. (2003). Dynamic causal modelling. *NeuroImage, 19*(4), 1273-1302. doi:10.1016/s1053-8119(03)00202-7

Friston, K. J., Kahan, J., Biswal, B. & Razi, A. (2014). A DCM for resting state fMRI. *NeuroImage, 94*(100), 396-407. doi:10.1016/j.neuroimage.2013.12.009

Friston, K. J., Mechelli, A., Turner, R. & Price, C. J. (2000). Nonlinear responses in fMRI: the Balloon model, Volterra kernels, and other hemodynamics. *NeuroImage, 12*(4), 466-477. doi:10.1006/nimg.2000.0630

Furchgott, R. F. (1983). Role of endothelium in responses of vascular smooth muscle. *Circulation research, 53*(5), 557-573. doi:10.1161/01.RES.53.5.557

Gauthier, C. J. & Fan, A. P. (2019). BOLD signal physiology: models and applications. *NeuroImage, 187*(1), 116-127. doi:10.1016/j.neuroimage.2018.03.018

Glasser, M. F., Sotiropoulos, S. N., Wilson, J. A., Coalson, T. S., Fischl, B., Andersson, J. L., . . . Polimeni, J. R. (2013). The minimal preprocessing pipelines for the Human Connectome Project. *NeuroImage, 80*, 105-124. doi:10.1016/j.neuroimage.2013.04.127

Goldstone, A., Mayhew, S. D., Przezdzik, I., Wilson, R. S., Hale, J. R. & Bagshaw, A. P. (2016). Gender specific re-organization of resting-state networks in older age. *Frontiers in aging neuroscience, 8*, 1-15. doi:10.3389/fnagi.2016.00285

González-Alonso, J., Mortensen, S. P., Dawson, E. A., Secher, N. H. & Damsgaard, R. (2006). Erythrocytes and the regulation of human skeletal muscle blood flow and oxygen delivery: role of erythrocyte count and oxygenation state of haemoglobin. *The Journal of physiology, 572*(1), 295-305. doi:10.1113/jphysiol.2005.101121

Greicius, M. D., Krasnow, B., Reiss, A. L. & Menon, V. (2003). Functional connectivity in the resting brain: a network analysis of the default mode hypothesis. *Proceedings of the National Academy of Sciences, 100*(1), 253-258. doi:10.1073/pnas.0135058100

Greicius, M. D., Srivastava, G., Reiss, A. L. & Menon, V. (2004). Default-mode network activity distinguishes Alzheimer's disease from healthy aging: evidence from functional MRI. *Proceedings of the National Academy of Sciences, 101*(13), 4637-4642. doi:10.1073/pnas.0308627101

Habas, C., Kamdar, N., Nguyen, D., Prater, K., Beckmann, C. F., Menon, V. & Greicius, M. D. (2009). Distinct cerebellar contributions to intrinsic connectivity networks. *Journal of Neuroscience, 29*(26), 8586-8594. doi:10.1523/JNEUROSCI.1868-09.2009

Hamilton, J. P., Farmer, M., Fogelman, P. & Gotlib, I. H. (2015). Depressive rumination, the default-mode network, and the dark matter of clinical neuroscience. *Biological psychiatry, 78*(4), 224-230. doi:10.1016/j.biopsych.2015.02.020

Handwerker, D. A., Gonzalez-Castillo, J., D'esposito, M. & Bandettini, P. A. (2012). The continuing challenge of understanding and modeling hemodynamic variation in fMRI. *NeuroImage, 62*(2), 1017-1023. doi:10.1016/j.neuroimage.2012.02.015

Harper, A. M. (1966). Autoregulation of cerebral blood flow: influence of the arterial blood pressure on the blood flow through the cerebral cortex. *Journal of neurology, neurosurgery, and psychiatry, 29*(5), 398-403. doi:10.1136/jnnp.29.5.398

Harrison, B. J., Pujol, J., Ortiz, H., Fornito, A., Pantelis, C. & Yücel, M. (2008). Modulation of brain resting-state networks by sad mood induction. *PloS one, 3*(3), 1-12. doi:10.1371/journal.pone.0001794

Heeger, D. J. & Ress, D. (2002). What does fMRI tell us about neuronal activity? *Nature reviews neuroscience, 3*(2), 142-151. doi:10.1038/nrn730

Herculano-Houzel, S. (2009). The human brain in numbers: a linearly scaled-up primate brain. *Frontiers in human neuroscience, 3*(31), 1-11. doi:10.3389/neuro.09.031.2009

Hodkinson, D. J., O'daly, O., Zunszain, P. A., Pariante, C. M., Lazurenko, V., Zelaya, F. O., . . . Williams, S. C. (2014). Circadian and homeostatic modulation of functional connectivity and regional cerebral blood flow in humans under normal entrained conditions. *Journal of Cerebral Blood Flow & Metabolism, 34*(9), 1493-1499. doi:10.1038/jcbfm.2014.109

Honey, C. J., Sporns, O., Cammoun, L., Gigandet, X., Thiran, J.-P., Meuli, R. & Hagmann, P. (2009). Predicting human resting-state functional connectivity from structural connectivity. *Proceedings of the National Academy of Sciences, 106*(6), 2035-2040. doi:doi.org/10.1073/pnas.0811168106

HumanConnectomeProject. (2013). WU-Minn HCP Consortium Open Access Data Use Terms. Retrieved from https://www.humanconnectome.org/study/hcp-young-adult/document/wu-minn-hcp-consortium-open-access-data-use-terms (22.04.2020)

HumanConnectomeProject. (2016). WU-Minn HCP Consortium Restricted Data Use Terms. Retrieved from https://www.humanconnectome.org/study/hcp-young-adult/document/wu-minn-hcp-consortium-restricted-data-use-terms (22.04.2020)

HumanConnectomeProject. (2017). 1200 Subject Data Release. Retrieved from https://www.humanconnectome.org/study/hcp-young-adult/document/1200-subjects-data-release

HumanConnectomeProject. (2018). HCP S1200 Release Referance Manual. Retrieved from https://www.humanconnectome.org/storage/app/media/documentation/s1200/HCP_S1200_Release_Reference_Manual.pdf (30.04.2020)

Iso, H., Kiyama, M., Naito, Y., Sato, S., Kitamura, A., Iida, M., . . . Komochi, Y. (1991). The relation of body fat distribution and body mass with haemoglobin A1c, blood pressure

and blood lipids in urban Japanese men. *International journal of epidemiology, 20*(1), 88-94. doi:10.1093/ije/20.1.88

Jae, S. Y., Kurl, S., Laukkanen, J. A., Heffernan, K. S., Choo, J., Choi, Y.-H. & Park, J. B. (2014). Higher blood hematocrit predicts hypertension in men. *Journal of hypertension, 32*(2), 245-250. doi:10.1097/HJH.0000000000000029

Kobuch, S., Macefield, V. G. & Henderson, L. A. (2019). Resting regional brain activity and connectivity vary with resting blood pressure but not muscle sympathetic nerve activity in normotensive humans: An exploratory study. *Journal of Cerebral Blood Flow & Metabolism, 39*(12), 2433-2444. doi:10.1177/0271678X18798442

Koechlin, E. & Summerfield, C. (2007). An information theoretical approach to prefrontal executive function. *Trends in cognitive sciences, 11*(6), 229-235. doi:10.1016/j.tics.2007.04.005

Krueger, S. & Nossal, R. (1988). SANS studies of interacting hemoglobin in intact erythrocytes. *Biophysical journal, 53*(1), 97-105. doi:10.1016/S0006-3495(88)83070-4

Kuczmarski, R. J. & Flegal, K. M. (2000). Criteria for definition of overweight in transition: background and recommendations for the United States. *The American journal of clinical nutrition, 72*(5), 1074-1081. doi:10.1093/ajcn/72.5.1074

Lalande, S., Hofman, P. & Baldi, J. (2010). Effect of reduced total blood volume on left ventricular volumes and kinetics in type 2 diabetes. *Acta physiologica, 199*(1), 23-30. doi:10.1111/j.1748-1716.2010.02081.x

Lam, B. C. C., Koh, G. C. H., Chen, C., Wong, M. T. K. & Fallows, S. J. (2015). Comparison of body mass index (BMI), body adiposity index (BAI), waist circumference (WC), waist-to-hip ratio (WHR) and waist-to-height ratio (WHtR) as predictors of cardiovascular disease risk factors in an adult population in Singapore. *PloS one, 10*(4), 1-15. doi:10.1371/journal.pone.0122985

Lassen, N. A. (1959). Cerebral blood flow and oxygen consumption in man. *Physiological reviews, 39*(2), 183-238. doi:10.1152/physrev.1959.39.2.183

Lee, M. H., Smyser, C. D. & Shimony, J. S. (2013). Resting-state fMRI: a review of methods and clinical applications. *American Journal of neuroradiology, 34*(10), 1866-1872. doi:10.3174/ajnr.A3263

Lemmens, H. J. M., Bernstein, D. P. & Brodsky, J. B. (2006). Estimating blood volume in obese and morbidly obese patients. *Obesity surgery, 16*(6), 773-776. doi:10.1381/096089206777346673

Levin, J. M., Frederick, B. d., Ross, M. H., Fox, J. F., von Rosenberg, H. L., Kaufman, M. J., . . . Renshaw, P. F. (2001). Influence of baseline hematocrit and hemodilution on BOLD fMRI activation. *Magnetic resonance imaging, 19*(8), 1055-1062. doi:10.1016/s0730-725x(01)00460-x

Liu, L., Li, W., Zhang, Y., Qin, W., Lu, S. & Zhang, Q. (2017). Weaker functional connectivity strength in patients with type 2 diabetes mellitus. *Frontiers in neuroscience, 11*(39), 1-11. doi:10.3389/fnins.2017.00390

Logothetis, N. K. & Wandell, B. A. (2004). Interpreting the BOLD signal. *Annu. Rev. Physiol., 66*(2004), 735-769. doi:10.1146/annurev.physiol.66.082602.092845

Manoliu, A., Riedl, V., Zherdin, A., Mühlau, M., Schwerthöffer, D., Scherr, M., . . . Bäuml, J. (2014). Aberrant dependence of default mode/central executive network interactions on anterior insular salience network activity in schizophrenia. *Schizophrenia bulletin, 40*(2), 428-437. doi:10.1093/schbul/sbt037

Maxwell, S. E., Lau, M. Y. & Howard, G. S. (2015). Is psychology suffering from a replication crisis? What does “failure to replicate” really mean? *American Psychologist, 70*(6), 487-498. doi:10.1037/a0039400

Menon, V. & Uddin, L. Q. (2010). Saliency, switching, attention and control: a network model of insula function. *Brain Structure and Function, 214*(5-6), 655-667. doi:10.1007/s00429-010-0262-0

Mevel, K., Chételat, G., Eustache, F. & Desgranges, B. (2011). The default mode network in healthy aging and Alzheimer's disease. *International journal of Alzheimer's disease, 2011*(special issue), 1-9. doi:10.4061/2011/535816

Murphy, K., Birn, R. M. & Bandettini, P. A. (2013). Resting-state fMRI confounds and cleanup. *NeuroImage, 2013*(80), 349-359. doi:10.1016/j.neuroimage.2013.04.001

Murphy, W. G. (2014). The sex difference in haemoglobin levels in adults—mechanisms, causes, and consequences. *Blood reviews, 28*(2), 41-47. doi:10.1016/j.blre.2013.12.003

Ogawa, S., Lee, T.-M., Kay, A. R. & Tank, D. W. (1990). Brain magnetic resonance imaging with contrast dependent on blood oxygenation. *Proceedings of the National Academy of Sciences, 87*(24), 9868-9872. doi:10.1073/pnas.87.24.9868

Park, H.-J., Friston, K. J., Pae, C., Park, B. & Razi, A. (2018). Dynamic effective connectivity in resting state fMRI. *NeuroImage, 180*, 594-608. doi:10.1016/j.neuroimage.2017.11.033

Paus, T. (2001). Primate anterior cingulate cortex: where motor control, drive and cognition interface. *Nature reviews neuroscience, 2*(6), 417-424. doi:10.1038/35077500

Payne, S. (2016). *Cerebral autoregulation: control of blood flow in the brain*: Springer.

Perutz, M. F., Rossmann, M. G., Cullis, A. F., Muirhead, H., Will, G. & North, A. (1960). Structure of hæmoglobin: a three-dimensional Fourier synthesis at 5.5-A. resolution, obtained by X-ray analysis. *Nature, 185*(4711), 416-422. doi:10.1038/185416a0

Pittman, R. N. (2011). *The circulatory system and oxygen transport*. San Rafael, CA: Morgan & Claypool Life Sciences. https://www.ncbi.nlm.nih.gov/books/NBK54104/

Poldrack, R. A. & Gorgolewski, K. J. (2014). Making big data open: data sharing in neuroimaging. *Nature neuroscience, 17*(11), 1510-1517. doi:10.1038/nn.3818

PsychInfo. (2019). Retrieved from http://ovidsp.dc1.ovid.com.pva.uib.no (22.03.2020)

PubMed. (2019). Retrieved from https://www.ncbi.nlm.nih.gov/pubmed/ (22.03.2020)

Raichle, M. E., MacLeod, A. M., Snyder, A. Z., Powers, W. J., Gusnard, D. A. & Shulman, G. L. (2001). A default mode of brain function. *Proceedings of the National Academy of Sciences, 98*(2), 676-682. doi:10.1073/pnas.98.2.676

Raichle, M. E. & Mintun, M. A. (2006). Brain work and brain imaging. *Annu. Rev. Neurosci., 29*, 449-476. doi:10.1146/annurev.neuro29.051605.112819

Rangaprakash, D., Wu, G. R., Marinazzo, D., Hu, X. & Deshpande, G. (2018). Hemodynamic response function (HRF) variability confounds resting-state fMRI functional connectivity. *Magnetic resonance in medicine, 80*(4), 1697-1713. doi:doi.org/10.1002/mrm.27146

Rudebeck, P. H., Behrens, T. E., Kennerley, S. W., Baxter, M. G., Buckley, M. J., Walton, M. E. & Rushworth, M. F. (2008). Frontal cortex subregions play distinct roles in choices between actions and stimuli. *Journal of Neuroscience, 28*(51), 13775-13785. doi:10.1523/JNEUROSCI.3541-08.2008

Sadler, J. R., Shearrer, G. E. & Burger, K. S. (2018). Body mass variability is represented by distinct functional connectivity patterns. *NeuroImage, 181*, 55-63. doi:0.1016/j.neuroimage.2018.06.082

Sadler, J. R., Shearrer, G. E. & Burger, K. S. (2019). Alterations in ventral attention network connectivity in individuals with prediabetes. *Nutritional neuroscience, 22*(4), 1-8. doi:10.1080/1028415X.2019.1609646

Sand, O., Sjaastad, Ø. V., Haug, E. & Bjålie, J. G. (2018). *Menneskekroppen, Fysiologi og anatomi* (3 ed.). Oslo: Gyldendal Akademisk.

Schmidek, H. H., Auer, L. M. & Kapp, J. P. (1985). The cerebral venous system. *Neurosurgery, 17*(4), 663-678. doi:10.1227/00006123-198510000-00024

Science, W. o. (2019). Retrieved from http://apps.webofknowledge.com.pva.uib.no/ (22.03.2020)

Seeley, W. W., Menon, V., Schatzberg, A. F., Keller, J., Glover, G. H., Kenna, H., . . . Greicius, M. D. (2007). Dissociable intrinsic connectivity networks for salience processing and executive control. *Journal of Neuroscience, 27*(9), 2349-2356. doi:10.1523/JNEUROSCI.5587-06.2007

Sheline, Y. I., Barch, D. M., Price, J. L., Rundle, M. M., Vaishnavi, S. N., Snyder, A. Z., . . . Raichle, M. E. (2009). The default mode network and self-referential processes in depression. *Proceedings of the National Academy of Sciences, 106*(6), 1942-1947. doi:10.1073/pnas.0812686106

Siegel, G. (1996). Vascular smooth muscle. In G. R & W. U (Eds.), *Comprehensive Human Physiology* (pp. 1941-1964): Springer, Berlin, Heidelberg.

Singh, K. D. & Fawcett, I. (2008). Transient and linearly graded deactivation of the human default-mode network by a visual detection task. *NeuroImage, 41*(1), 100-112. doi:10.1016/j.neuroimage.2008.01.051

Smith, J. E. (1987). Erythrocyte Membrane: Structure, Function, and Pathophysiology. *Veterinary pathology, 24*(6), 471-476. doi:10.1177/030098588702400601

Smith, S. M. & Nichols, T. E. (2018). Statistical challenges in “big data” human neuroimaging. *Neuron, 97*(2), 263-268. doi:10.1016/j.neuron.2017.12.018

Snyder, A. Z. & Raichle, M. E. (2012). A brief history of the resting state: the Washington University perspective. *NeuroImage, 62*(2), 902-910. doi:10.1016/j.neuroimage.2012.01.044

Snyder, G. & Sheafor, B. (2015). Red Blood Cells: Centerpiece in the Evolution of the Vertebrate Circulatory System. *American zoologist, 39*(2), 189-198. doi:10.1093/icb/39.2.189

Specht, K. (2019). Current challenges in translational and clinical fMRI and future directions. *Frontiers in Psychiatry, 10*, 1-9. doi:10.3389/fpsyt.2019.00924

Sridharan, D., Levitin, D. J. & Menon, V. (2008). A critical role for the right fronto-insular cortex in switching between central-executive and default-mode networks. *Proceedings of the National Academy of Sciences, 105*(34), 12569-12574. doi:10.1073/pnas.0800005105

Stadler, A. M., Digel, I., Artmann, G., Embs, J. P., Zaccai, G. & Büldt, G. (2008). Hemoglobin dynamics in red blood cells: correlation to body temperature. *Biophysical journal, 95*(11), 5449-5461. doi:10.1529/biophysj.108.138040

Stephan, K. E., Penny, W. D., Moran, R. J., den Ouden, H. E., Daunizeau, J. & Friston, K. J. (2010). Ten simple rules for dynamic causal modeling. *NeuroImage, 49*(4), 3099-3109. doi:10.1016/j.neuroimage.2009.11.015

Stephens, R., B. & Stilwell, D., L. (1969). *Arteries and veins of the human brain*. Springfield, Illinnois, USA: Charles C. Thomas.

Strandgaard, S. & Paulson, O. B. (1984). Cerebral autoregulation. *Stroke, 15*(3), 413-416. doi:10.1161/01.STR.15.3.413

Sætrevik, B. & Peterson, Å. (2017). Replikasjons krisen. *Tidsskrift for Norsk psykologforening, 54*(7), 641-647. Retrieved from https://psykologtidsskriftet.no/fagessay/2017/07/replikasjonskrisen

Tak, S., Wang, D. J., Polimeni, J. R., Yan, L. & Chen, J. J. (2014). Dynamic and static contributions of the cerebrovasculature to the resting-state BOLD signal. *NeuroImage, 84*(1), 672-680. doi:10.1016/j.neuroimage.2013.09.057

Tan, C. O., Hamner, J. & Taylor, J. A. (2013). The role of myogenic mechanisms in human cerebrovascular regulation. *The Journal of physiology, 591*(20), 5095-5105. doi:10.1113/jphysiol.2013.259747

Tankova, T., Chakarova, N., Dakovska, L. & Atanassova, I. (2012). Assessment of HbA1c as a diagnostic tool in diabetes and prediabetes. *Acta diabetologica, 49*(5), 371-378. doi:doi.org/10.1007/s00592-011-0334-5

Toro, R., Fox, P. T. & Paus, T. (2008). Functional coactivation map of the human brain. *Cerebral Cortex, 18*(11), 2553-2559. doi:10.1093/cercor/bhn014

Tucker, W. D. & Mahajan, K. (2018). *Anatomy, blood vessels*. Treasure Island (FL): StatPearls Publishing.

Turner, B. O., Paul, E. J., Miller, M. B. & Barbey, A. K. (2018). Small sample sizes reduce the replicability of task-based fMRI studies. *Communications Biology, 1*, 1-10. doi:10.1038/s42003-018-0073-z

U.K, B. (2014). About UK Biobank. Retrieved from https://www.ukbiobank.ac.uk/about-biobank-uk (15.04.2020)

Uğurbil, K., Xu, J., Auerbach, E. J., Moeller, S., Vu, A. T., Duarte-Carvajalino, J. M., . . . Van de Moortele, P. F. (2013). Pushing spatial and temporal resolution for functional and diffusion MRI in the Human Connectome Project. *NeuroImage, 80*, 80-104. doi:10.1016/j.neuroimage.2013.05.012

Van Den Heuvel, M. P. & Pol, H. E. H. (2010). Exploring the brain network: a review on resting-state fMRI functional connectivity. *European neuropsychopharmacology, 20*(8), 519-534. doi:10.1016/j.euroneuro.2010.03.008

Van Essen, D. C., Smith, S. M., Barch, D. M., Behrens, T. E. J., Yacoub, E. & Ugurbil, K. (2013). The WU-Minn Human Connectome Project: An overview. *NeuroImage, 80*, 62-79. doi:10.1016/j.neuroimage.2013.05.041

Van Essen, D. C., Ugurbil, K., Auerbach, E., Barch, D., Behrens, T., Bucholz, R., . . . Curtiss, S. W. (2012). The Human Connectome Project: a data acquisition perspective. *NeuroImage, 62*(4), 2222-2231. doi:10.1016/j.neuroimage.2012.02.018

Waites, A. B., Stanislavsky, A., Abbott, D. F. & Jackson, G. D. (2005). Effect of prior cognitive state on resting state networks measured with functional connectivity. *Human brain mapping, 24*(1), 59-68. doi:0.1002/hbm.20069

Walsh, M. P. (1994). Regulation of vascular smooth muscle tone. *Canadian journal of physiology and pharmacology, 72*(8), 919-936. doi:10.1139/y94-130

Weiland, B. J., Sabbineni, A., Calhoun, V. D., Welsh, R. C., Bryan, A. D., Jung, R. E., . . . Hutchison, K. E. (2014). Reduced left executive control network functional connectivity is associated with alcohol use disorders. *Alcoholism: Clinical and Experimental Research, 38*(9), 2445-2453. doi:10.1111/acer.12505

Whittaker, J. R., Driver, I. D., Venzi, M., Bright, M. G. & Murphy, K. (2019). Cerebral autoregulation evidenced by synchronized low frequency oscillations in blood pressure and resting-state fMRI. *Frontiers in neuroscience, 13*, 1-12. doi:10.3389/fnins.2019.00433

Woodward, N. D., Rogers, B. & Heckers, S. (2011). Functional resting-state networks are differentially affected in schizophrenia. *Schizophrenia research, 130*(3), 86-93. doi:10.1016/j.schres.2011.03.010

Xu, F., Li, W., Liu, P., Hua, J., Strouse, J. J., Pekar, J. J., . . . Qin, Q. (2018). Accounting for the role of hematocrit in between-subject variations of MRI-derived baseline cerebral hemodynamic parameters and functional BOLD responses. *Human brain mapping, 39*(1), 344-353. doi:10.1002/hbm.23846

Yang, S. Q., Xu, Z. P., Zhan, Y. F., Guo, L. Y., Zhang, S., Jiang, R. F., . . . Wang, J. Z. (2016). Altered intranetwork and internetwork functional connectivity in type 2 diabetes

mellitus with and without cognitive impairment. *Scientific reports, 6*, 1-11. doi:10.1038/srep32980

Yang, Z., Craddock, R. C. & Milham, M. P. (2015). Impact of hematocrit on measurements of the intrinsic brain. *Frontiers in neuroscience, 8*, 1-10. doi:10.3389/fnins.2014.00452

Zeidman, P., Jafarian, A., Corbin, N., Seghier, M. L., Razi, A., Price, C. J. & Friston, K. J. (2019). A tutorial on group effective connectivity analysis, part 1: first level analysis with DCM for fMRI. *NeuroImage, 200*, 174-190. doi:10.1016/j.neuroimage.2019.06.032

Zeidman, P., Jafarian, A., Seghier, M. L., Litvak, V., Cagnan, H., Price, C. J. & Friston, K. J. (2019). A guide to group effective connectivity analysis, part 2: Second level analysis with PEB. *NeuroImage, 200*, 12-25. doi:10.1016/j.neuroimage.2019.06.031

Zhao, J. M., Clingman, C. S., Närväinen, M. J., Kauppinen, R. A. & van Zijl, P. C. (2007). Oxygenation and hematocrit dependence of transverse relaxation rates of blood at 3T. *Magnetic Resonance in Medicine: An Official Journal of the International Society for Magnetic Resonance in Medicine, 58*(3), 592-597. doi:10.1002/mrm.21342

Zhu, D. C., Tarumi, T., Khan, M. A. & Zhang, R. (2015). Vascular coupling in resting-state fMRI: evidence from multiple modalities. *Journal of Cerebral Blood Flow & Metabolism, 35*(12), 1910-1920. doi:10.1038/jcbfm.2015.166

Appendix A

Literature Search

Search Engines

The search engines Pub Med (2019), Psych Info (2019), and Web of Science (2019) were considered as adequate, as they cover a range of literature from the fields of psychology, neuroscience and medicine.

Strategy

Search word combinations of each term related to the independent variables (Table 1) in combination with at least one term related to the dependent variables (Table 2), using the search engine function "AND".

Selection of Relevant Papers

The selections of scientific papers was made with regards to its relevance to this thesis. Articles that were highly related to diseases were therefore not included. For example, paper including "blood pressure", but with a focus on stroke or thrombosis were not included; papers including "erythrocytes" or "hematocrit", but with a focus on kidney failure or sickle cell anemia were not included. An exception was made for searches including "long-term blood sugar/glycated hemoglobin", that was related to diabetes. The remaining search hits were examined and included in this thesis based on their relevance. The literature search was conducted from 20th September to 30th October, 2019.

Table A.1

Search Words Related to the Independent Variables

Independent Variable	Synonyms	Related Terms	Abbreviation
Blood Pressure	Arterial Blood Pressure	Hypertensive; Normotensive	BP
Hematocrit	Red Blood Cells; Red Blood Cell Count; Red Cells; Erythrocytes		HCT
Body Mass	Body Mass Index	Weight	BMI
Long-term Blood Sugar	Glycated Hemoglobin; Glycohemoglobin	Diabetes	HbA1c

Note. Terms related to the independent variables, their synonyms, related terms or abbreviations.

Table A.2

Search Words Related to the Dependent Variables

Dependent Variable	Synonyms	Related Terms	Abbreviation
Resting State Functional Magnetic Resonance Imaging	Resting State; Resting State fMRI	Resting State Network	RS-fMRI; Resting fMRI; Rest fMRI,
Default Mode Network			DMN
Central Executive Network		Extrinsic Network	CEN
Salience Network			SN
Blood Oxygen Level Dependent Signal		BOLD alteration*s; BOLD variation*s; Hemodynamic Response	BOLD
Dynamic Causal Modelling		Effective Connectivity	DCM
Functional Connectivity			FC

Note. Terms related to the dependent variables, their synonyms, related terms or abbreviations.

Appendix B

Ethical Approval

REK
REGIONALE KOMITEER FOR MEDISINSK OG HELSEFAGLIG FORSKNINGSETIKK

Region:	Saksbehandler:	Telefon:	Vår dato:	Vår referanse:
REK vest	Camilla Gjerstad		13.12.2019	31972
			Deres referanse:	

Karsten Specht

31972 ReState

Forskningsansvarlig: Universitetet i Bergen

Søker: Karsten Specht

Søkers beskrivelse av formål:

As recently recognised, the entire field of psychology suffers from the "replication crisis". The general perception of this problem is that studies in psychology and neuroimaging suffer substantially from a lack of statistical power, meaning that the sample sizes are typically too small, and effect sizes are too low. However, one may ask the question whether this is really the case or whether one should try to convert the critically seen variability into the signal of interest by asking the question: What is the origin of this variability?
The primary purpose of this project is to identify possible (bio-)markers that may cause either variability in neuronal activity or in the vascular system since both have an indistinguishable influence on the fMRI signal.
With the help of open-access databases and the collection of fMRI data and blood- and saliva samples, possible candidates for causes of variability should be identified, and guidelines for future fMRI studies will be developed.

REKs vurdering

Vi viser til søknad om forhåndsgodkjenning av ovennevnte forskningsprosjekt. Søknaden ble behandlet av Regional komité for medisinsk og helsefaglig forskningsetikk (REK vest) i møtet 27.11.19. Vurderingen er gjort med hjemmel i helseforskningsloven § 10.

Språk
Søknadsskjemaet skulle vært utfylt på norsk. REK vest vil likevel behandlet søknaden

ettersom REK-portalen frem til nå har manglet informasjon om krav til norsk språk. Vi ber imidlertid om at evt. neste søknad til REK fylles ut på norsk dersom studien foregår i Norge.

Studiepopulasjon
60 friske forskningsdeltakere vil bli inkluderte i studien.

Metode
I følge søknaden er formålet i studien er å forbedre påliteligheten til metodene som brukes i hjerneavbildningsstudier. I studien vil man skanne deltakerne i maskinen flere ganger med ulike fremgangsmåter. I skanneren vil deltaker få ulike oppmerksomhetsoppgaver og språklige oppgaver. I tillegg vil man ta spytt- og blodprøver underveis i studien. Totalt vil deltaker skannes fire ganger med ulike mellomrom fra noen dager til flere uker. Validerte spørreskjema vil bli benyttet (Edinburgh Handendess- Myers-Briggs Type Indicator-Pittsburgh Sleep Quality Index Logbook on sleeping quality and eating behaviour).

Studien vil i tillegg benyttes tidligere registrerte opplysninger fra fire internasjonale databaser (Human Connectom Project, UK Biobank, Alzheimer's Disease Neuroimaging Initiative, The Autism Brain Imaging Data Exchange). Man ønsker å foreta en sammenstilling av opplysninger fra de ulike registre ved å benytte maskinlæring. Hensikten er å korrelere nevroavbildningsdata med visse biomarkører (hematokrit, BMI, kjønn, kjønnshormoner). REK vest oppfatter søknaden det slik at det kun er snakk om å bruke reelt anonyme data fra disse fire databasene, der det ikke er mulig å identifisere enkeltpersoner direkte eller indirekte.

Forsvarlighetsvurdering
Deltakerne vil være utstyrt med en nødknapp mens de er inne i MR-maskinen. Det vil bli tatt tre blodprøver per MR-økt. MR-data vil bli undersøkt av radiolog. Bergen fMRI-gruppe har etablert prosedyrer for tilfeldige funn: Først vil radiologen kontakte den ansvarlige forskeren for å diskutere de videre prosedyrene, og deretter blir deltakeren bedt om å kontakte radiologen. Avhengig av hvilken type funn, vil oppfølging videre gis enten direkte av sykehuset, eller deltakerne vil bli henvist til fastlegen. Komiteen har ingen merknader til dette.

Rekruttering
Studien vil rekruttere deltakere gjennom annonser ved Haukeland universitetssjukehus/Universitetet i Bergen og via sosiale medier. Deltakelse i studien vil bli kompensert med gavekort på 200 NOK for hver MR-undersøkelse. Komiteen diskuterte om beløpet er en tilstrekkelig kompensasjon for tidsbruken i studien. REK vest ber prosjektgruppen vurdere om det kan gis mer betaling til deltakerne. Vi ber om tilbakemelding om dette.

Informasjonsskriv
Komiteen har følgende merknader til informasjonsskrivet:

- Deltakelsen innebærer omfattende testing, og dette underkommuniseres noe i skrivet. Dette må kommuniseres tydeligere som en mulig ulempe.
- Tittel på informasjonsskrivet «Å løse replikasjonskrisen» er noe vidløftig og bør endres/neddempes.
- Følgende setning må omformuleres: «*Mine anonymiserte og avidentifiserte dataen kan deles» til «Mine anonyme data kan deles.»*
- Noen tunge formuleringer i skrivet bør forenkles. Teksten bør språkvaskes, f.eks.: … *en navneliste som kun eksitere på papir …, (…) Vi er dermed ute etter å se vi både på hjernens anatomiske struktur.*

Biobank
Prøver som skal analyseres i studien er spyttprøver, serum, plasma, DNA ekstrahert og RNA ekstrahert. Prøvene vil lagres i en spesifikk forskningsbiobank knyttet til prosjektet. Oppgitt ansvarshavende for biobanken er Karsten Specht.

Ifølge helseforskningsloven § 26 må ansvarshavende være en person med medisinsk eller biologisk utdanning av høyere grad. REK vest forutsetter at angitt ansvarshavende har slik kompetanse.

Genetiske undersøkelser
Det vil bli gjennomført genetiske undersøkelser i studien. Studien er eksplorerende, og søker mener at det ikke er sannsynlig at prosjektet vil generere tilsiktet eller utilsiktet prediktiv geninformasjon som vil kunne gi helsegevinst til enkeltdeltakere.

Dataoppbevaring
Data/prøver vil være indirekte identifiserbare og det opprettes en koblingsnøkkel. Alle data vil bli lagret på forskningsserveren SAFE.

Prosjektslutt
Prosjektslutt: 31.12.2024. Søker bekrefter at etter prosjektslutt vil koblingsnøkkel oppbevares i inntil fem år for kontrollhensyn. Deretter skal en eventuell kodenøkkel slettes og materialet slettes eller anonymiseres.

Søker bekrefter at ved prosjektslutt vil biologisk materiale benyttet i studien bli destruert. REK vest har ingen merknader til dette.

Datadeling
Ifølge søknaden vil ingen rådata bli gjort tilgjengelig for andre. Søker peker på at datadeling kan være nødvendig. REK vest forutsette at det kun er snakk om deling av reelt anonyme data, der det ikke er mulig å bakveisidentifisere enkeltpersoner, verken direkte eller indirekte.

Vedtak

Godkjent med vilkår

Vilkår

- Revidert informasjonsskriv må sendes til REK vest.
- REK vest ber prosjektgruppen vurdere om det kan gis mer betaling til deltakerne og gi tilbakemelding om dette.

Svar sendes via REK-portalen (se oppgaver).

REK vest har gjort en helhetlig forskningsetisk vurdering av alle prosjektets sider. Prosjektet godkjennes med hjemmel i helseforskningsloven § 10 på betingelse av ovennevnte vilkår.

Sluttmelding
Søker skal sende sluttmelding til REK vest på eget skjema senest seks måneder etter godkjenningsperioden er utløpt, jf. hfl. § 12.

Søknad om å foreta vesentlige endringer
Dersom man ønsker å foreta vesentlige endringer i forhold til formål, metode, tidsløp eller organisering, skal søknad sendes til den regionale komiteen for medisinsk og helsefaglig forskningsetikk som har gitt forhåndsgodkjenning. Søknaden skal beskrive hvilke endringer som ønskes foretatt og begrunnelsen for disse, jf. hfl. § 11.

Klageadgang
Du kan klage på komiteens vedtak, jf. forvaltningsloven § 28 flg. Klagen sendes til REK vest. Klagefristen er tre uker fra du mottar dette brevet. Dersom vedtaket opprettholdes av REK vest, sendes klagen videre til Den nasjonale forskningsetiske komité for medisin og helsefag (NEM) for endelig vurdering.

Appendix C

Inclusion and Exclusion Criteria

Table B.1

Inclusion and Exclusion Criteria

HCP Inclusion Criteria	**1.** Age 22 to 35 at the time of telephone diagnostic interview (SSAGA) **2.** Ability to give valid informed consent
HCP Exclusion Criteria	**1**. Significant history of psychiatric disorder, substance abuse, neurological, or cardiovascular disease: a. Participant report of diagnosis by treating physician; or b. Hospitalization for the condition for two days or longer; or c. Pharmacological or behavioral treatment by cardiologist, psychiatrist, neurologist, or endocrinologist for a period of 12 months or longer, other than treatment for childhood-only ADHD **2.** Two or more seizures after age 5 or a diagnosis of epilepsy **3.** Any genetic disorder, such as cystic fibrosis or sickle cell disease **4.** Multiple sclerosis, cerebral palsy, brain tumor or stroke **5.** Any of the following head injuries: a. Loss of consciousness for >30 minutes; or b. Amnesia for >24 hours; or c. Change in mental status for >24 hours; or d. CT findings consistent with traumatic brain injury; or e. Three or more concussive (mild) incidences of head injury **6.** Premature birth (for twins, before 34 weeks; for non-twin siblings, before 37 weeks. If weeks unknown, less than 5 Ibs. at birth for non-twins) **7.** Currently on chemotherapy or immunomodulatory agents, or history of radiation or chemotherapy that could affect the brain **8.** Thyroid hormone treatment in the past **9.** Treatment for diabetes in the past month (other than gestational or diet-controlled diabetes) **10.** Use of daily prescription medication for migraines in the past month **11.** A score of 25 or below on the Folstein Mini Mental State Exam (Folstein, Folstein, & McHugh, 1975) on visit Day 1 **12.** Moderate or severe claustrophobia **13.** Pregnancy **14.** Unsafe metal in the body

Note. Meeting any single exclusion criterion is sufficient for the participant to be excluded from the study, although prospective participants who are pregnant may be re-contacted after their due dates. Reproduced from Van Essen et al. (2013).

Appendix D

Human Connectome Project, Data Collection

Table D.1

HCP Data Collection: SSAGA Telephone Diagnostic Interview Categories

Collected Data	Specificities
Demographics. Education, employment and income. Physical and mental health history. Present and past use of tobacco, alcohol, marijuana and other drugs.	
Symptoms/ history of:	Eating disorders. Depression. Suicidality. Psychosis. Anti-social personality. Obsessive-compulsive disorder. Post-traumatic stress. Social phobia. Panic attacks.

Note. The categories covered in the telephone interview, which was used to access if the subjects met the inclusion/ exclusion criteria. SSAGA = Semi-Structured Assessment for the Genetics of Alcoholism. Reproduced from (Van Essen et al., 2013)

Table D.2

HCP Data Collection: Procedures during subject visits Day 1

Procedure	Involving	Specificities
Intake procedure:	Review/sign Informed Consent.	
	Folstein Mini Mental State Exam.	
	Pittsburgh Sleep Quality Index.	
	Parental psychiatric and neurologic history.	
	Handedness assessment.	
	Menstrual cycle and other endocrine information in females.	
	Urine drug screen.	
	Breathalyzer test.	
	MRI safety screening.	
	Blood drawn for:	Thyroid stimulating hormone.
		Hemoglobin A1c.
		Genotyping.
		Hematocrit.
Mock scanner practice.		
Structural MRI.		
NIH Toolbox behavioral tests.		
Functional MRI session 1:	30 minutes resting-state MRI.	
	30 minutes task-activated MRI.	
Recognition task (outside of scanner)		

Note. Order of procedures conducted at day 1 at the research facility. The order may have varied in some cases due to quality or scheduling issues. Reproduced from Van Essen et al. (2013).

Table D.3

HCP Data Collection: Procedures during subject visits Day 2

Procedure	Involving
Diffusion MRI. Non-toolbox behavioral tests.	
Functional MR session 2:	30 minutes resting-state MRI. 30 minutes task-activated MRI.
Exit procedure:	7-day retrospective smoking and alcohol questionnaire. Urine drug screen. Breathalyzer test. Participant satisfaction survey.

Note. Order of procedures conducted at day 2 at the research facility. The order may have varied in some cases due to quality or scheduling issues. Reproduced from Van Essen et al. (2013).

Appendix E

Descriptive Statistics for the Dependent Variables / DCM Parameters

Table E.1

Descriptive Statistics for the Hemodynamic Parameter Transit Time

			Mean				
Transit Time	Min.	Max.	Statistic	Std. Error	SD	Skewness	Kurtosis
PCC	-.6811	.4676	-.2174	.008	.212	.544	-.036
mPFC	-.6961	.6822	-.1350	.010	.244	.383	.046
LIPC	-.5861	.6992	-.0628	.008	.205	.469	.555
RIPC	-.5753	.6762	-.0394	.008	.200	.469	.519
AI	-.5116	.8459	.1023	.008	.205	.113	.132
ACC	-.7864	.6854	-.1620	.010	.253	.266	-.161
DLPFC	-.5983	.6650	-.0181	-.018	.198	.492	.694
PPC	-.7495	.6161	-.1019	-.007	.186	.367	.762

Note. The descriptive statistics for the dependent variables *transit time*. N = 594. Kurtosis std. error: .200, Skewness std. error: .100. Min. = minimum score; Max. = maximum score; Std. Error = standard error; SD = standard deviation. PCC = posterior cingulate cortex; mPFC = medial prefrontal cortex; LIPC/RIPC = left/right inferior parietal cortex; AI = anterior insula; ACC = anterior cingulate cortex; DLPFC = dorsolateral prefrontal cortex; PPC = posterior parietal cortex.

Table E.2

Descriptive Statistics for the Hemodynamic Parameters Epsilon and Decay

			Mean				
	Min.	Max.	Statistic	Std. Error	SD	Skewness	Kurtosis
Epsilon	-.8932	.0409	-.4228	.007	.176	-.214	-.071
Decay	-1.0603	-.0548	-.4152	.006	.155	-.845	1.108

Note. The descriptive statistics for the dependent variables *epsilon* and *decay*. N = 594. Kurtosis std. error: .200, Skewness std. error: .100. Min. = minimum score; Max. = maximum score; Std. Error = standard error; SD = standard deviation.

Table E.3

Descriptive Statistics for the Effective Connectivity Parameters: Connections from PCC

			Mean				
	Min.	Max.	Statistic	Std. Error	SD	Skewness	Kurtosis
PCC	-1.1707	.6829	-.1358	.012	.315	-.247	.040
PCC to mPFC	-1.0639	.7800	.0625	.011	.270	-.257	.762
PCC to LIPC	-.8266	.5291	.0219	.007	.190	-.570	1.515
PCC to RIPC	-.8747	.5272	.0091	.006	.162	-.641	2.424
PCC to AI	-.7895	.6140	-.0122	.007	.177	-.324	1.683
PCC to ACC	-.9475	.7251	-.0263	.007	.191	-.151	1.453
PCC to DLPFC	-.4752	.5229	.0002	.005	.131	.139	1.571
PPC to PPC	-.4930	.4554	-.0148	.005	.127	.160	1.263

Note. The descriptive statistics for the dependent variable effective connectivity, showing connections from PCC. N = 594. Kurtosis std. error: .200, Skewness std. error: .100. Min. = minimum score; Max. = maximum score; Std. Error = standard error; SD = standard deviation. PCC = posterior cingulate cortex; mPFC = medial prefrontal cortex; LIPC/RIPC = left/right inferior parietal cortex; AI = anterior insula; ACC = anterior cingulate cortex; DLPFC = dorsolateral prefrontal cortex; PPC = posterior parietal cortex.

Table E.4

Descriptive Statistics for the Effective Connectivity Parameters: Connections from mPFC

			Mean				
	Min.	Max.	Statistic	Std. Error	SD	Skewness	Kurtosis
mPFC	-1.4819	.5672	-.3372	.013	.335	-.296	.208
mPFC to PCC	-.9166	.7917	.1062	.008	.215	-.206	.887
mPFC to LIPC	-.5863	.6232	.0327	.006	.153	.066	1.648
mPFC to RIPC	-.4538	.5507	.0501	.005	.139	.232	.821
mPFC to AI	-.7582	.6072	.0848	.007	.178	-.172	1.320
mPFC to ACC	-.5437	1.0057	.1483	.009	.222	.334	.631
mPFC to DLPFC	-.6354	.6273	.0283	.005	.141	.221	2.239
mPFC to PPC	-.4388	.4818	.0069	.005	.124	.284	.885

Note. The descriptive statistics for the dependent variable effective connectivity, showing connections from mPFC. N = 594. Kurtosis std. error: .200, Skewness std. error: .100. Min. = minimum score; Max. = maximum score; Std. Error = standard error; SD = standard deviation. PCC = posterior cingulate cortex; mPFC = medial prefrontal cortex; LIPC/RIPC = left/right inferior parietal cortex; AI = anterior insula; ACC = anterior cingulate cortex; DLPFC = dorsolateral prefrontal cortex; PPC = posterior parietal cortex.

.

Table E.5

Descriptive Statistics for the Effective Connectivity Parameters: Connections from LIPC

			Mean				
	Min.	Max.	Statistic	Std. Error	SD	Skewness	Kurtosis
LIPC	-.8843	1.1050	.0645	.013	.320	-.249	.136
LIPC to PCC	-.8454	.9961	.1445	.011	.278	-.125	.230
LIPC to mPFC	-.9001	.8693	.0296	.011	.278	-.256	.658
LIPC to RIPC	-.7183	.6025	.0513	.007	.191	-.297	.554
LIPC to AI	-.6936	.7769	-.0717	.008	.200	.417	1.463
LIPC to ACC	-.8154	.7658	-.0996	.009	.222	-.273	.632
LIPC to DLPFC	-.7766	.5195	-.0155	.007	.179	-.330	1.114
LIPC to PPC	-.6302	.4318	-.0236	.006	.162	-.072	.462

Note. The descriptive statistics for the dependent variable effective connectivity, showing connections from LIPC. N = 594. Kurtosis std. error: .200, Skewness std. error: .100. Min. = minimum score; Max. = maximum score; Std. Error = standard error; SD = standard deviation. PCC = posterior cingulate cortex; mPFC = medial prefrontal cortex; LIPC/RIPC = left/right inferior parietal cortex; AI = anterior insula; ACC = anterior cingulate cortex; DLPFC = dorsolateral prefrontal cortex; PPC = posterior parietal cortex.

Table E.6

Descriptive Statistics for the Effective Connectivity Parameters: Connections from RIPC

			Mean				
	Min.	Max.	Statistic	Std. Error	SD	Skewness	Kurtosis
RIPC	-1.0866	1.1307	.1509	.012	.308	-.507	1.038
RIPC to PCC	-.7393	.9318	.1257	.010	.248	-.273	.552
RIPC to mPFC	-.7690	.8497	.0606	.010	.252	-.017	.564
RIPC to LIPC	-.5956	.6360	.0875	.008	.201	-.249	.000
RIPC to AI	-.6694	.5639	-.0678	.007	.185	.033	.709
RIPC to ACC	-1.1458	.4397	-.1021	.008	.218	-.345	.842
RIPC to DLPFC	-.7277	.5916	.0426	.007	.192	-.333	.939
RIPC to PPC	-.6445	.7737	.0840	.007	.183	-.102	.963

Note. The descriptive statistics for the dependent variable effective connectivity, showing connections from RIPC. N = 594. Kurtosis std. error: .200, Skewness std. error: .100. Min. = minimum score; Max. = maximum score; Std. Error = standard error; SD = standard deviation. PCC = posterior cingulate cortex; mPFC = medial prefrontal cortex; LIPC/RIPC = left/right inferior parietal cortex; AI = anterior insula; ACC = anterior cingulate cortex; DLPFC = dorsolateral prefrontal cortex; PPC = posterior parietal cortex.

Table E.7

Descriptive Statistics for the Effective Connectivity Parameters: Connections from AI

			Mean				
	Min.	Max.	Statistic	Std. Error	SD	Skewness	Kurtosis
AI	-1.2199	.6252	-.2797	.013	.332	-.109	-.088
AI to PCC	-.9809	.6630	-.1654	.010	.257	-.075	.248
AI to mPFC	-1.0665	.8207	-.0525	.012	.297	-.095	.128
AI to LIPC	-.9157	.4327	-.1055	.008	.209	-.465	.707
AI to RIPC	-1.0439	.5689	-.0767	.007	.188	-.564	1.964
AI to ACC	-.6283	1.2406	.2982	.011	.278	-.153	.609
AI to DLPFC	-.6372	.9710	.0767	.007	.177	-.306	1.658
AI to PPC	-.8426	.5807	.0725	.007	.173	-.501	1.705

Note. The descriptive statistics for the dependent variable effective connectivity, showing connections from AI. N = 594. Kurtosis std. error: .200, Skewness std. error: .100. Min. = minimum score; Max. = maximum score; Std. Error = standard error; SD = standard deviation. PCC = posterior cingulate cortex; mPFC = medial prefrontal cortex; LIPC/RIPC = left/right inferior parietal cortex; AI = anterior insula; ACC = anterior cingulate cortex; DLPFC = dorsolateral prefrontal cortex; PPC = posterior parietal cortex.

Table E.8

Descriptive Statistics for the Effective Connectivity Parameters: Connections from ACC

			Mean				
	Min.	Max.	Statistic	Std. Error	SD	Skewness	Kurtosis
ACC	-1.1251	.5098	-.1990	.011	.275	-.263	-.180
ACC to PCC	-.9539	.9123	.0368	.008	.209	-.182	2.668
ACC to mPFC	-.7632	1.0503	.0900	.010	.244	.314	.886
ACC to LIPC	-1.0034	.6134	.0286	.006	.157	-.583	4.668
ACC to RIPC	-.6324	.5985	.0262	.005	.138	-.305	2.143
ACC to AI	-.5506	.8813	.0098	.008	.218	.333	.153
ACC to DLPFC	-.5961	.5868	.0382	.006	.155	.014	1.257
ACC to PPC	-.5154	.7082	.0659	.006	.146	.214	1.298

Note. The descriptive statistics for the dependent variable effective connectivity, showing connections from ACC. N = 594. Kurtosis std. error: .200, Skewness std. error: .100. Min. = minimum score; Max. = maximum score; Std. Error = standard error; SD = standard deviation. PCC = posterior cingulate cortex; mPFC = medial prefrontal cortex; LIPC/RIPC = left/right inferior parietal cortex; AI = anterior insula; ACC = anterior cingulate cortex; DLPFC = dorsolateral prefrontal cortex; PPC = posterior parietal cortex.

Table E.9

Descriptive Statistics for the Effective Connectivity Parameters: Connections from DLPFC

			Mean				
	Min.	Max.	Statistic	Std. Error	SD	Skewness	Kurtosis
DLPFC	-.8548	1.1005	.1257	.012	.312	-.303	-.097
DLPFC to PCC	-1.0218	.9809	-.0074	.009	.230	.072	1.480
DLPFC to mPFC	-1.0460	.8583	-.0470	.010	.253	.234	1.104
DLPFC to LIPC	-.5734	.6808	.1032	.008	.199	-.121	.051
DLPFC to RIPC	-.4337	.6383	.1140	.007	.185	-.240	.077
DLPFC to AI	-.5909	.8097	.0287	.008	.206	.097	.623
DLPFC to ACC	-.5918	.6822	-.0309	.008	.209	-.008	.262
DLPFC to PPC	-.4706	.7428	.1877	.009	.222	-.312	.022

Note. The descriptive statistics for the dependent variable effective connectivity, showing connections from DLPFC. N = 594. Kurtosis std. error: .200, Skewness std. error: .100. Min. = minimum score; Max. = maximum score; Std. Error = standard error; SD = standard deviation. PCC = posterior cingulate cortex; mPFC = medial prefrontal cortex; LIPC/RIPC = left/right inferior parietal cortex; AI = anterior insula; ACC = anterior cingulate cortex; DLPFC = dorsolateral prefrontal cortex; PPC = posterior parietal cortex.

Table E.10

Descriptive Statistics for the Effective Connectivity Parameters: Connections from PPC

			Mean				
	Min.	Max.	Statistic	Std. Error	SD	Skewness	Kurtosis
PPC	-.9775	.9725	.2047	.011	.276	-.352	.296
PPC to PCC	-.8858	.5725	-.1357	.008	.208	-.245	.769
PPC to mPFC	-1.0837	.4252	-.1965	.010	.248	-.573	.380
PPC to LIPC	-.6648	.6261	-.0168	.007	.187	-.283	.522
PPC to RIPC	-.7820	.5797	.0325	.007	.185	-.349	.922
PPC to AI	-.9241	.6630	-.0554	.008	.209	-.112	1.087
PPC to ACC	-1.1046	.6763	-.1151	.009	.238	.065	.657
PPC to DLPFC	-.6515	.7184	-.0666	.008	.213	-.145	.125

Note. The descriptive statistics for the dependent variable effective connectivity, showing connections from PPC. Kurtosis std. error: .200, Skewness std. error: .100. Min. = minimum score; Max. = maximum score; Std. Error = standard error; SD = standard deviation. PCC = posterior cingulate cortex; mPFC = medial prefrontal cortex; LIPC/RIPC = left/right inferior parietal cortex; AI = anterior insula; ACC = anterior cingulate cortex; DLPFC = dorsolateral prefrontal cortex; PPC = posterior parietal cortex.

Table E.11

Descriptive Statistics for the csd Parameters: α- and β-values

			Mean				
	Min.	Max.	Statistic	Std. Error	SD	Skewness	Kurtosis
α	-2.7100	.4115	-.8147	.021	.515	-.999	1.132
β	-1.3568	-.1.2213	-.3952	.019	.472	.700	.565

Note. The descriptive statistics for the dependent variables csd parameters. N = 594. Kurtosis std. error: .200, Skewness std. error: .100. Min. = minimum score; Max. = maximum score; Std. Error = standard error; SD = standard deviation; α = α-value; β = β-value.

Table E.12

Descriptive Statistics for the Free Energy Parameter

			Mean				
	Min.	Max.	Statistic	Std. Error	SD	Skewness	Kurtosis
Free Energy	-6051.02	5238.63	1165.83	63.70	1552.72	-.729	1.275

Note. The descriptive statistics for the dependent variable Free Energy. N = 594. Kurtosis std. error: .200, Skewness std. error: .100. Min. = minimum score; Max. = maximum score; Std. Error = standard error; SD = standard deviation.

Appendix F

Correlation Matrix for the Independent Variables

Table F.1

Correlation Matrix for the Correlation between the Independent Variables

		BMI	HbA1c	HCT	Sys BP	Dia BP
BMI	Pearson Correlation	1	.050	.030	.335	.291
	Sig.		.312	.491	.000**	.000**
	N	593	417	547	589	589
HbA1c	Pearson Correlation	.050	1	-.045	.063	.062
	Sig.	.312		.363	.203	211
	N	417	417	412	414	414
HCT	Pearson Correlation	.030	-.045	1	.105*	.085
	Sig.	.491	.363		.015	.048*
	N	547	412	547	543	543
Sys BP	Pearson Correlation	.335	.063	.105	1	.680
	Sig.	.000**	.203	.015*		.000**
	N	589	414	543	590	590
Dia BP	Pearson Correlation	.291	.062	.085	.680	1
	Sig.	.000**	.211	.048*	.000**	
	N	589	414	543	590	590

Note. Correlations between the independent variables BMI, HbA1c, HCT, systolic and diastolic BP. BMI = Body Mass Index, HbA1c = glycated hemoglobin; HCT = hematocrit; Sys BP = systolic blood pressure; Dia BP = diastolic blood pressure.

*Sig. two-tailed $p < .05$, **Sig. two-tailed $p < .01$.

Appendix G

Regression Tables for Effective Connectivity Parameters

Regression Tables for effective connectivity parameters were the outcome variables were the not significantly predicted by BP, HCT, BMI or HbA1c (G.1); where the independent variables did not contribute significantly to explaining the variance in the outcome variable (G.2); or were the full models were not significant (G.3).

Table G.1

Effective Connectivity Parameters sig. Predicted by Gender Alone

	Modell Summary						Coefficients	
	Model	R^2	R^2 Change	(df reg, df res) = F	Sig.	Sig. F Change	*beta*	Sig.
PCC to AI	Gender	.011		(1,575) = 6.615	.010**			
	Gender	.021	.010		.016*	.128	-.097	.027*
	Dia BP			(4,572) =			-.057	.324
	Sys BP			3.088			.014	.815
	BMI						-.074	.100
mPFC to AI	Gender	.008		(1,579) = 4.578	.033*			
	Gender	.013	.005		.025*	.093	.084	.043*
	BMI			(2,578) =			.070	.093
				3.714				
LIPC to PCC	Gender	.009		(1,576) = 5.143	.024*			
	Gender	.015	.006		.036*	.180	-.071	.103
	Dia BP			(3,574) =			-.023	.696
	Sys BP			2.800			-.063	.298
RIPC to ACC	Gender	.008		(1,576) = 4.517	.034*			
	Gender	.020	.012		.010**	.032*	-.054	.215
	Dia BP			(3,574) =			-.012	.840
	Sys BP			3.829			-.106	.079

Note. Effective connectivity parameters that were significantly predicted by gender alone. As can be seen from Sig. F Change, the independent variables did not make a significant contribution to explaining the variance in the outcome variables, except for in RIPC to ACC, but for this regression none of the independent variables made a

unique significant contribution. Dia BP = diastolic blood pressure; Sys BP = systolic blood pressure; BMI = Body Mass Index; PCC = posterior cingulate cortex; AI = anterior insula; mPFC = medial prefrontal cortex; LIPC/RIPC = left/right inferior parietal cortex; ACC = anterior cingulate cortex; df reg = *degrees of freedom* regression; df res = *degrees of freedom* residual; *beta* = standardized coefficient beta.

*$p < .05$, **$p < .01$.

Table G.2

Effective Connectivity Parameters not sig. Predicted by the Full Model

	Modell Summary						Coefficients	
	Model	R^2	R^2 Change	(df reg, df res) = F	Sig.	Sig. F Change	*beta*	Sig.
PCC to mPFC	Gender	.000		(1,576) = .095	.758			
	Gender	.008	.008		.090	.030*	-.016	.710
	Sys BP			(2,575) = 2.417			.095	.030*
mPFC to RIPC	Gender	.000		(1,579) = .002	.962			
	Gender	.010	.010		.062	.018*	-.005	.910
	BMI			(2,578) = 2.800			.098	.018*
mPFC to ACC	Gender	.001		(1,579) = .734	.392			
	Gender	.009	.007		.080	.038*	.030	.474
	BMI			(2,578) = 2.543			.087	.038*
RIPC to PPC	Gender	.001		(1,576) = .434	.510			
	Gender	.010	.009		.057	.021*	-.012	.771
	Dia BP			(2,575) = 2.887			-.097	.021*
DLPFC to AI	Gender	.000		(1,576) = .003	.957			
	Gender	.008	.008		.113	.037*	-.012	.784
	Dia BP			(2,575) = 2.191			.088	.037*
ACC to PPC	Gender	.000		(1,410) = .056	.813			
	Gender	.009	.009		.276	.149	-.014	.783
	BMI			(3,408) = 1.294			.073	.141
	HbA1c						.054	.280

Note. Effective connectivity parameters were the full models were not significantly explaining the variance of the outcome variables. For all the regressions except for ACC to PPC the independent variables contributed to explaining more of the variance than gender alone. Dia BP = diastolic blood pressure; Sys BP = systolic blood pressure; BMI = Body Mass Index; HbA1c = glycated hemoglobin; PCC = posterior cingulate cortex; AI = anterior insula; mPFC = medial prefrontal cortex; RIPC = right inferior parietal cortex; ACC = anterior cingulate cortex; DLPFC = dorsolateral prefrontal cortex; PPC = posterior parietal cortex; df reg = *degrees of freedom* regression; df res = *degrees of freedom* residual; *beta* = standardized coefficient beta. *$p < .05$, **$p < .01$.

Table G.3

Effective Connectivity Parameters sig. Predicted by the Full Model, without any of the Independent Variables Making a Unique Contribution to Explaining the Variance

	Modell Summary					Coefficients	
	Model	R^2	R^2 Change	(df reg, df res) = F	Sig.	Sig. F Change	*beta*	Sig.
AI to ACC	Gender	.000		(1,569) = .005	.945			
	Gender	.014	.014		.047*	.019*	.027	.537
	Dia BP			(3,574) =			-.098	.092
	Sys BP			2.666			-.028	.638
AI to DLPFC	Gender	.001		(1,576) = .492	.483	.012*		
	Gender	.016	.015		.025*		.067	.124
	Dia BP			(3,574) =			-.022	.705
	Sys BP			3.138			-.113	.061
AI to PPC	Gender	.006		(1,407) = 2.639	.105			
	Gender	.040	.034		.005**	.007**	.119	.022
	Dia BP			(5,403) =			-.109	.114
	Sys BP			3.381			-.071	.330
	BMI						-.034	.527
	HbA1c						-.041	.410

Note. Effective connectivity parameters were the full models were significantly explaining the variance of the outcome variables, and the independent variables explained significantly more than gender alone, but none of the independent variables made a unique significant contribution. Dia BP = diastolic blood pressure; Sys BP = systolic blood pressure; BMI = Body Mass Index; HbA1c = glycated hemoglobin; AI = anterior insula; ACC = anterior cingulate cortex; DLPFC = dorsolateral prefrontal cortex; PPC = posterior parietal cortex; df reg = *degrees of freedom* regression; df res = *degrees of freedom* residual; *beta* = standardized coefficient beta.

*$p < .05$, **$p < .01$.

Appendix H

Frequency Distribution of BMI Groups

Figure H.1

Frequency Distribution for BMI Groups

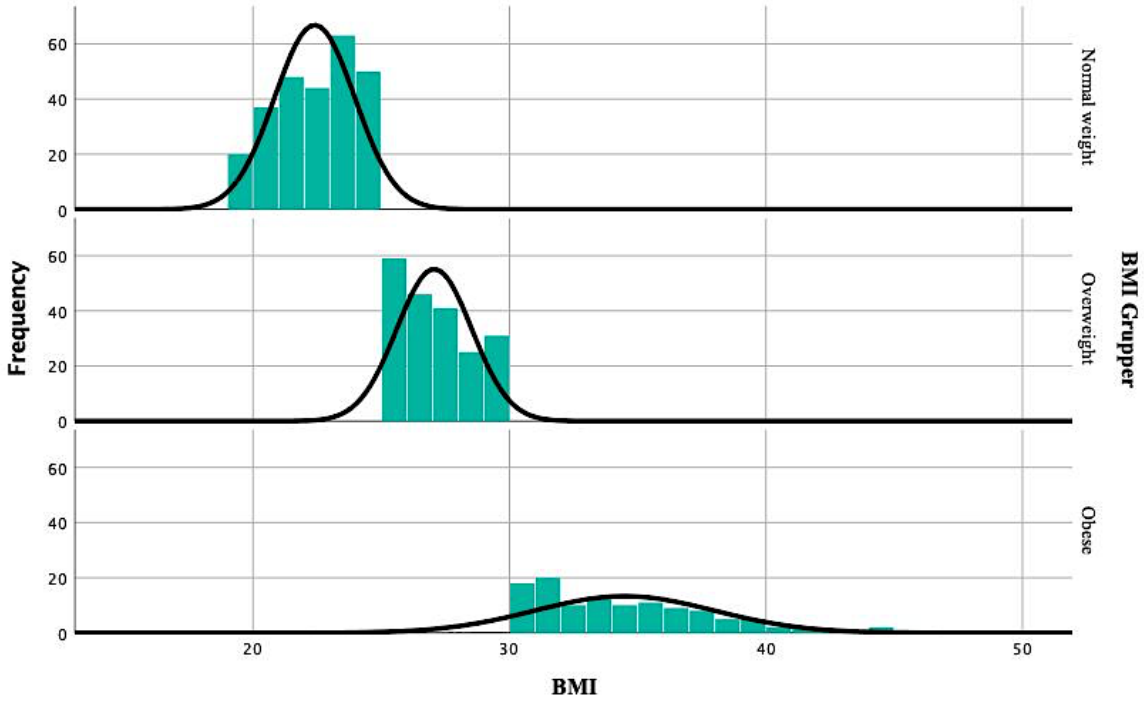

Note. Exhibits the non-normal distribution of BMI, and that the shape of the distribution is not similar across the groups. Normal weight (19-24 kg., N=262), Overweight (25-29 kg., N=202) and Obese (>30 kg., N=117).

Appendix I

Results of the Kruskal-Wallis H Test for Hemodynamic Parameters

Table I.1

Kruskal-Wallis H Tests with the Hemodynamic Parameters

	Kruskal – Wallis H Test		Pairwise Comparisons				
Parameter	Sig.	Chi [2]	Pairwise Comparison	Std. Stat.	Adj.Sig	*r*	Mean Rank
PCC *transit time*	.013*	8.718	NW – OB OW – OB NW – OW	1.841 2.952 -1.349	.197 .009** .009	.165	NW: 292.61 OW: 314.00 OB: 258.66
mPFC *transit time*	.056[a]	5.750	.		.		.
LIPC *transit time*	.208	3.138	.		.		.
RIPC *transit time*	.856	.310	.		.		.
AI *transit time*	.646	.875	.		.		.
ACC *transit time*	.230	2.938	.		.		.
DLPFC *transit time*	.466	1.527	.		.		.
PPC *transit time*	.458	1.560	.		.		.
Decay	.904	.201	.		.		.
Epsilon	.267	2.875	.		.		.

Note. Kruskal Wallis H Test for between BMI group differences in the hemodynamic parameters. Normal Weight (19-24 kg., N = 262), overweight (25-29 kg., N = 202) and obese (>30 kg., N = 117), Total N = 585, *Degrees of Freedom* = 2. Std. Stat. = Standardized test statistic. Adj.Sig is the significance level after adjusting the alpha-value for multiple comparisons, with Bonferroni Corrections. *r* = effect size. Dash indicates no data obtained, as the pairwise comparison was not run. PCC = posterior cingulate cortex; mPFC = medial prefrontal cortex; LIPC/ RIPC = left / right inferior parietal cortex; AI = anterior insula; ACC = anterior cingulate cortex; DLPFC = dorsolateral prefrontal cortex; PPC = posterior parietal cortex; NW = normal weight; OW = overweight; OB = obese.

*p = .05, ** p = .01. [a] Close to significant group differences for mPFC *transit time*.

Appendix J

Non-significant Kruskal-Wallis H Tests for Effective Connectivity Parameters

Table J.1

Non-significant Between BMI Group Differences for Effective Connectivity Parameters

Connections	Sig.	Chi ^{2}
PCC	.398	1.846
PCC to LIPC	.284	2.519
PCC to AI	.314	2.319
PCC to ACC	.127	4.125
PCC to PPC	.691	.744
mPFC	.818	.401
mPFC to PCC	.461	1.550
mPFC to LIPC	.199	3.225
mPFC to AI	.446	1.616
mPFC to ACC	.257	2.716
mPFC to DLPFC	.157	3.697
mPFC to PPC	.214	3.084
LIPC to AI	.792	.467
LIPC to ACC	.993	.014
LIPC to DLPFC	.586	1.069
LIPC to PPC	.328	2.231
RIPC to PCC	.717	.666
RIPC mPFC	.824	.386
RIPC to LIPC	.944	.115
RIPC to AI	.507	1.358
RIPC to ACC	.065	5.478
RIPC to DLPFC	.648	.868
RIPC to PPC	.671	.797
AI	.709	.688
AI to PCC	.567	1.136
AI to LIPC	.917	.173
AI to RIPC	.627	.934
AI to ACC	.861	.300
AI to DLPFC	.957	.088
AI to PPC	.096	4.683
ACC	.368	2.001
ACC to PCC	.474	1.494
ACC to mPFC	.138	3.965
ACC to LIPC	.871	.275
ACC to RIPC	.288	2.491
ACC to AI	.446	1.614
ACC to DLPFC	.775	.509
ACC to PPC	.196	3.255
DLPFC	.648	.867
DLPFC to PCC	.233	2.916
DLPFC to mPFC	.199	3.230
DLPFC to LIPC	.080	5.043
DLPFC to RIPC	.198	3.243
DLPFC to AI	.570	1.125

DLPFC to ACC	.127	4.132
DLPFC to PPC	.694	.730
PPC	.124	4.174
PPC to PCC	.092	4.779
PPC to mPFC	.720	.656
PPC to LIPC	.315	2.308
PPC to RIPC	.834	.363
PPC to AI	.059	5.674
PPC to ACC	.900	.210
PPC to DLPFC	.661	.829

Note. Normal Weight (19-24 kg., N = 262), overweight (25-29 kg., N = 202) and obese (>30 kg., N = 117), Total N= 585, *degrees of freedom* = 2. PCC = posterior cingulate cortex; mPFC = medial prefrontal cortex; LIPC/ RIPC = left / right inferior parietal cortex; AI = anterior insula; ACC = anterior cingulate cortex; DLPFC = dorsolateral prefrontal cortex; PPC = posterior parietal cortex.

Appendix K

Frequency Distribution of Sibling Status

Table K.1

Frequency Distribution of Sibling Status

	Frequency
Monozygotic twin	178
Heterozygotic twin	123
Not twin	291

Note. Distribution of the forms of relation between the subjects in the study sample (N = 594).